UNIVERSITY OF OKLAHOMA

GRADUATE COLLEGE

STRUCTURAL SURVEY OF THE WOODFORD SHALE AT MCALISTER CEMETERY QUARRY, CARTER COUNTY, OKLAHOMA

A THESIS

SUBMITTED TO THE GRADUATE FACULTY

in partial fulfillment of the requirements for the

Degree of

MASTER OF SCIENCE

By

COLLEEN M. KLOCKOW
Norman, Oklahoma
2017

STRUCTURAL SURVEY OF THE WOODFORD SHALE AT MCALISTER CEMETERY QUARRY,
CARTER COUNTY, OKLAHOMA

A THESIS APPROVED FOR THE
CONOCOPHILLIPS SCHOOL OF GEOLOGY AND GEOPHYSICS

BY

_____
Dr. Roger M. Slatt, Chair

_____
Dr. Ze'ev Reches

_____
Dr. Matthew J. Pranter

Acknowledgements

I would like to thank my parents, Gary and Debra Klockow, for all of their support during my years of college. As I grew they were my inspiration, reinforcing my respect for their intelligence and drive year after year. I would also like to thank my siblings, Mike and Kim Klockow, for also showing me what can be achieved within this generation, and paving the way for my own adventures. I would also like to thank them for keeping me humble, as siblings do. Then I would like to thank my husband, Jonathan Buening, for remaining by my side since the very beginning of our adventure into the field of Geology. He has been my support through recent tough times, and a sounding board for advice when I am struggling.

Very importantly, I would like to thank my advisor Dr. Roger Slatt, for pointing the way in this final stage of my academic career and showing me the process behind a large scale research project. Without him I would have been most utterly lost.

Finally, I would like to thank the other members of my committee, Dr. Ze'ev Reches and Dr. Matthew Pranter, for their patient advice and help along the way.

There have been many other people that have helped me along the way as well, too many to name individually. This includes those such as professors from my undergrad, high school teachers who encouraged my early growth, and so on. To all of those people, I also extend my thanks.

Table of Contents

List of Figures

Abstract

The focus of this thesis is creating a geologic map of the Woodford Shale in McAlister Cemetery Quarry, and providing data indicating how the bitumen in fractures came to be in this location. Prior studies have focused on defining the stratigraphy of the Woodford within the quarry, agreeing on at least three distinct segments: the Upper, Middle, and Lower Woodford.

Key results of this thesis include a map of the quarry created using newly acquired GPS points noting the locations of significant structures, landmarks, and contacts as well as an analysis of thin sections taken from samples within the quarry. Contacts between beds were mapped using a combination of data from Andrea Serna's thesis and new GPS data. Initially this meant that the Upper, Middle, and Lower Woodford were 95, 133, and 144 feet thick, however part way through mapping, the definition of the boundary between the Middle and Upper Woodford was changed based on the first appearance of phosphate nodules. With this change, the Middle Woodford thickened to approximately 185 feet thick, and the Upper Woodford thinned to approximately 92 feet thick.

While gathering data for the geologic map, measurements of the mounds in the center of the quarry were taken to ascertain whether or not the mounds were *in situ* or were piles of debris from quarrying activities. Most of the mounds were *in situ*, with the only exception being the circular portion of the southernmost tip of the mounds, which can be seen on the map near the intersection of the gravel roads.

Faulting and folding within the quarry was investigated and what structures are currently visible in the quarry were documented. This included a NW trending fault

which can be seen on the North Wall of the quarry, and a series of folds visible on the Eastern Wall, including a syncline, an anticline, and an overturned syncline.

Thin sections were taken from samples from the Middle Woodford and analyzed for a mineralogical evaluation and to confirm the hypothesis that the mounds are *in situ*. Thin sections displayed fractures occasionally infilled with bitumen and calcite. In at least one instance, the bitumen infill was observed cutting through a calcite filled fracture while taking advantage of a previous plane of weakness, indicating that the event which created the bitumen-filled fractures happened after the event which created the calcite-filled fractures. In addition, all five samples displayed graded bedding, indicating sediment gravity flow and not suspension settling.

Introduction

Located near Ardmore, Oklahoma, McAlister Cemetery Quarry contains a clear exposure of the three commonly agreed upon units of the Woodford Shale: the Upper, Middle, and Lower Woodford. As such it has been the focus of numerous geologic studies, typically focusing on defining the characteristics of each unit. However, due to the past quarrying activities, some doubt has been thrown on exactly how undisturbed the rock is within the quarry.

Mounds of shale, apparently forming a clear section of the Middle Woodford, are nonetheless mostly covered in rubble, and on first glance seem to have either been faulted in the past or damaged by digging machines. Clearer outcrops of rock on a wall tracing down the eastern portion of the quarry and another cutting through the northern portion of the quarry show signs of structures including faults and/or folds, but it is not immediately clear which structure is visible in each location.

These structures are important to take into account as bitumen-filled fractures are scattered on various exposed surfaces within the quarry and questions remain as to how those hydrocarbons came to be there. One idea spurring this thesis was the question of whether a fault running through the quarry created a migration pathway for the hydrocarbons. As such, this thesis is focused on creating a geologic map of the quarry to be included in continuing Woodford studies, in order to help determine how much apparent damage is natural or man-made, as well as provide data indicating how the hydrocarbons came to be in this location. Many previous studies of the Woodford have been completed at the University of Oklahoma. These studies have included geologic characterizations (Serna-Bernal, 2013), seismic interpretations (Gupta, 2012;

Infante-Paez, 2015), sequence stratigraphic interpretations (Chain, 2012; Killian, 2012; Mann, 2014; McCullough, 2014), geochemical analysis (Miceli-Romero, 2010), geomechanical analysis (Tran, 2009), fracture analysis (Portas, 2009; Badra, 2011), palynomorphs (Molinares, 2013), and chemostratigraphic analysis (Treanton, 2014; Ekwunife, 2016; Turner, 2016).

Area of Study

This thesis covers the structural geology within the McAlister Cemetery Quarry, located near Ardmore, Oklahoma, as seen in Figure 1. The predominant formation contained within the quarry is the Woodford Shale, in addition to exposures of the Hunton Limestone and the Sycamore Limestone. Previous studies by the Institute of Reservoir Characterization (IRC) have noted various methods of subdividing the Woodford Shale, however the most commonly cited subdivisions in the literature regarding the Woodford Shale are the Lower, Middle, and Upper Woodford. These subdivisions were defined using well logs from West Texas (Ellison, 1950) and as such are not likely to be accurate descriptors for the Woodford in regions throughout Oklahoma due to potential differences in lithostratigraphy (Turner, 2016). In addition, these terms violate stratigraphic naming practices (Zalasiewicz et al, 2004). For these reasons, Turner suggests that they be used as proper nouns, and so they will appear capitalized throughout this work.

Other notable subdivisions of the Woodford completed by studying the formation in Oklahoma include the system devised by Killian, which divided the Woodford into 5 separate units characterized by their drilling properties (Killian, 2012), as well as the work done by Turner (2016), which defined 8 separate lithofacies within

the Woodford. However, it is important to state that Turner did not propose new unit names, instead describing different changes in lithofacies throughout the Upper, Middle, and Lower Woodford (Turner, 2016).

Despite these difficulties, the three units of the Woodford can be generally described. According to McCullough (2014), the Lower Woodford has the smallest aerial extent, and is thought to have been deposited proximally to the shoreline of the Paleotethys Seaway during its transgression. The Middle Woodford has the greatest aerial extent, and the highest gamma ray values and TOC (Total Organic Content). Finally, the Upper Woodford has the lowest TOC, contains phosphate nodules, and is thought to have been deposited proximally to the Paleotethys (McCullough, 2014). In his discussion of the lithofacies in the Woodford, Turner (2016) noted that the dominant lithofacies in the Lower Woodford is laminated shale, while the Middle Woodford is defined by a transition from laminated shale to black shale. The Upper Woodford has zones of phosphate nodules which grade into laminated shales (Turner, 2016).

Serna-Bernal (2013) defined a stratigraphic framework for the Woodford Shale within the quarry itself, citing the existence of all three units within the quarry (Serna-Bernal, 2013). These definitions have since been adjusted by Ekwunife and are now defined in Figures 2 and 3 (Ekwunife, 2016).

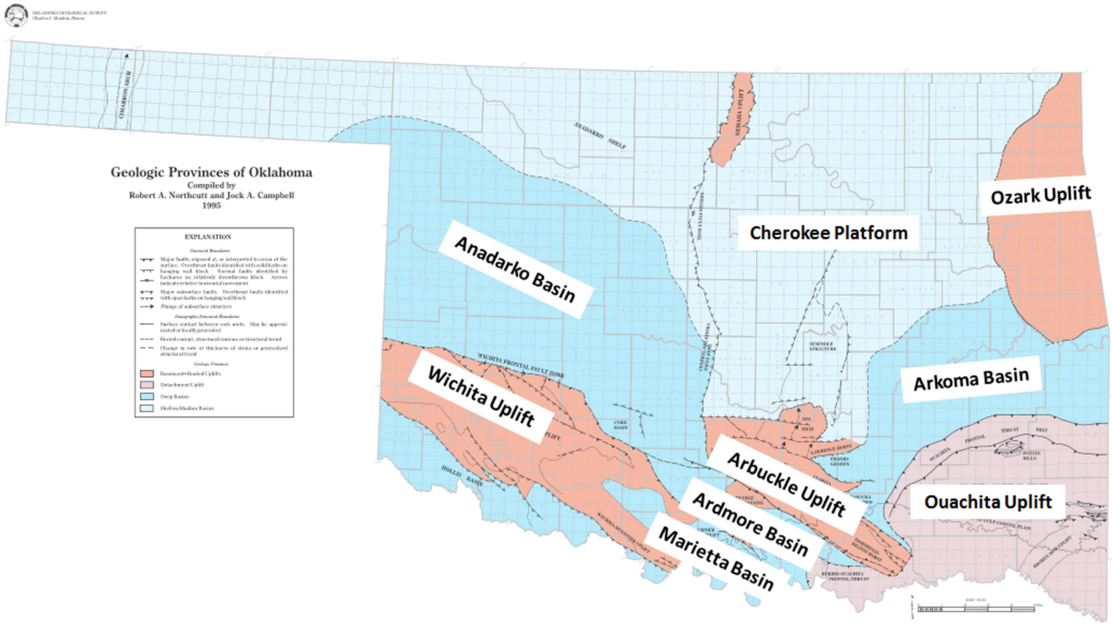

Figure 1 Geologic Regions of Oklahoma (Modified from Northcutt and Campbell, 1995).

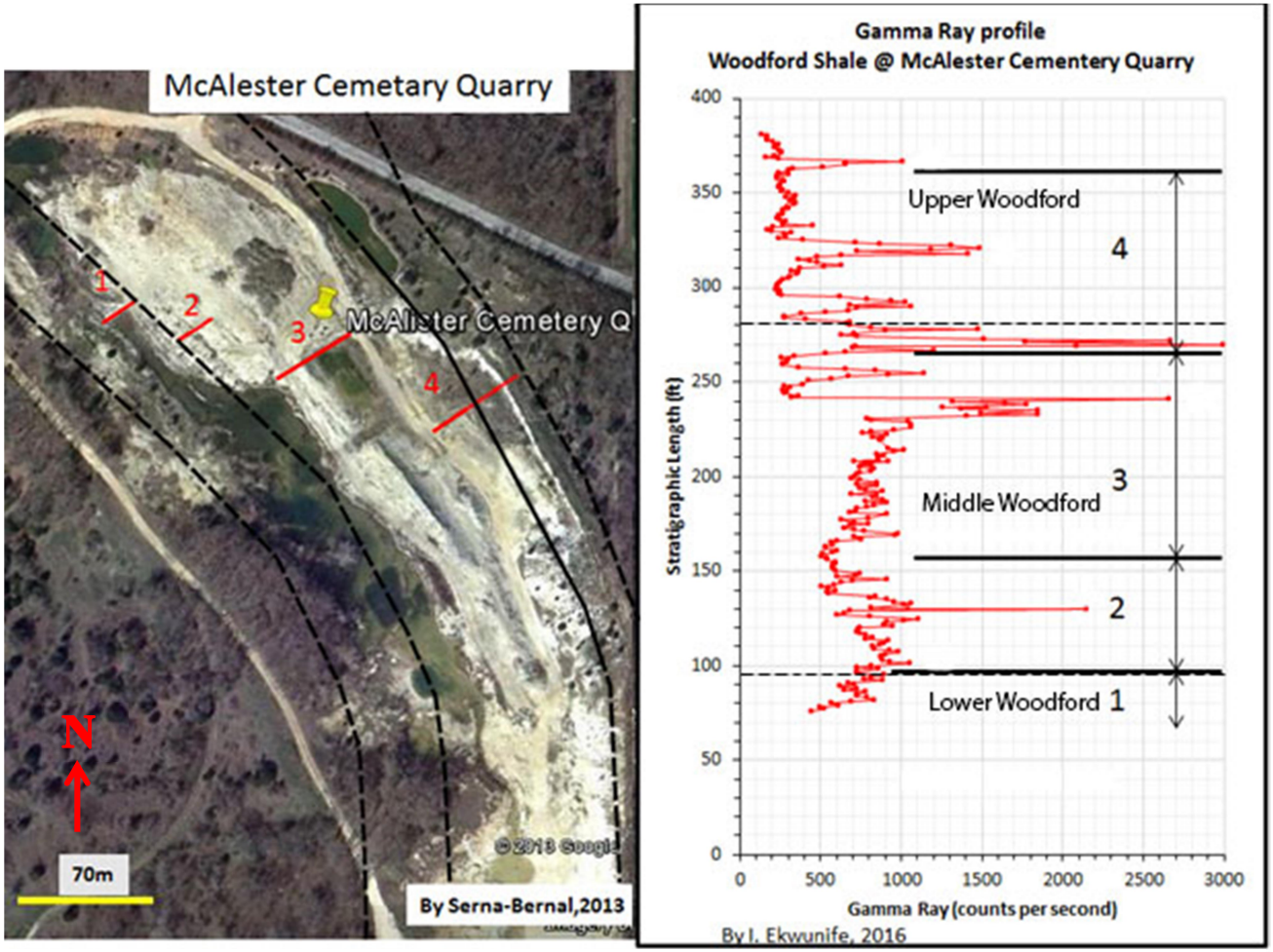

Figure 2 Gamma ray outcrop profile in counts/sec paired with an aerial view of McAlister Cemetery Quarry. Measurements taken along lines marked 1-4 (Figure Credit: Serna-Bernal, 2013; Ekwunife, 2016)

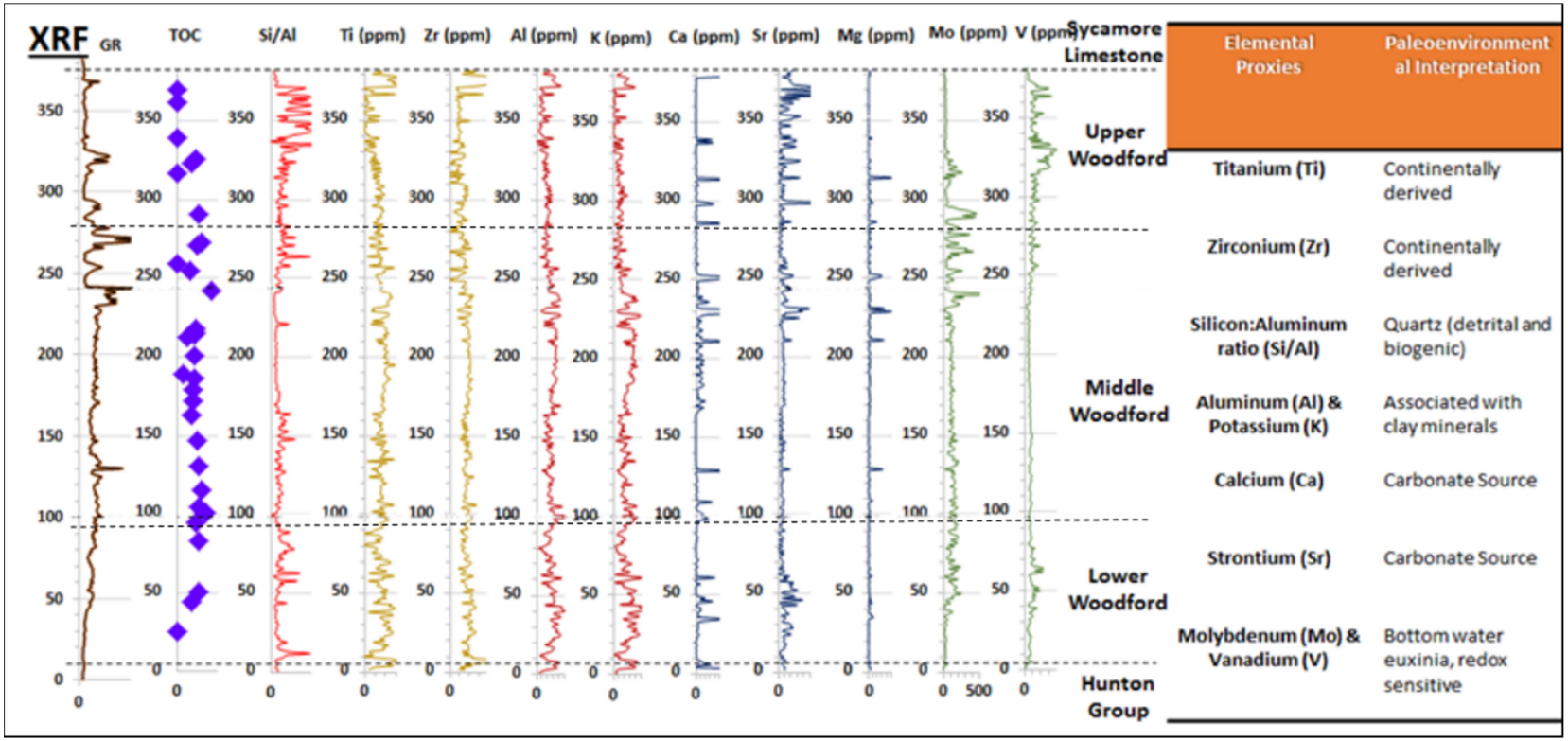

Figure 3 Chemostratigraphic profile showing XRF signals along the measured section from McAlister Cemetery Quarry as seen in Figure 2. The x axis shows Gamma Ray (GR), TOC, and elements measured in ppm, while the y axis shows measured depth in feet from the base to the top of the Woodford. Figure to the right describes potential paleoenvironmental interpretations of the XRF signals (Modified from Ekwunife, 2016).

In her thesis, Serna-Bernal measured the thickness of the Woodford within the quarry to be 372 feet thick. She then subdivided that into the Lower, Middle, and Upper Woodford, which she defined as being 95 feet, 133 feet, and 144 feet thick in that order (Serna-Bernal, 2013). The location at which Serna-Bernal defined the contact between the Upper and Middle Woodford can be found using a radiolarian rich white marker bed which outcropped twice during the course of fieldwork for this study, once at the north end of the quarry and once at the south. Due to the condition of the shale in the quarry, it is possible that either of these outcroppings is covered with debris at this point, however they could be found again in that case using the map provided and some digging tools.

During the course of her thesis, Serna-Bernal characterized the various strata within the quarry using multiple techniques. These included thin section and XRD analysis, Scanning Electron Microscope (SEM), and Gamma Ray Parasequences. In this way she characterized the Lower Woodford as containing two different lithofacies: laminated finely crystalline dolomite and laminated siliceous shale (Serna-Bernal, 2013). The Lower Woodford also contains two microfabric types identified through SEM: “organic hash” and “organic clayey”. She defined organic hash as organic matter where the mineral flakes are uneven, whereas she defined the organic clayey microfabric as having sharp edged mineral flakes. According to Serna-Bernal, the Woodford Shale was deposited during a second order sea level cycle, which is defined as lasting approximately 22 Ma. The Lower Woodford was deposited during a TST, and contains numerous 3rd order HST and TSTs (0.5-5 Ma) (Mitchum & Van Wagoner, 1990; Serna-Bernal, 2013).

Serna-Bernal describes the Middle Woodford as containing three lithofacies: laminated siliceous shale, laminated siliceous siltstone, and laminated finely crystalline dolomite. The Middle Woodford also contains two types of microfabric: organic hash and organic clayey. It was deposited during a transition from TST to HST (Serna-Bernal, 2013). Finally, Serna-Bernal defined the Upper Woodford as containing two lithofacies: laminated siliceous shale and laminated chert. It was deposited during an HST (Serna-Bernal, 2013).

The quarry, named for a cemetery located across the D3265 Road, is seemingly abandoned. Efforts to locate the current owners have only recently succeeded. Because of this, certain suggested methods of studying the quarry, including things such as obtaining a core sample, will need to be delayed until the proper owners can give permission for such a study. Survey work within the quarry was accomplished in the course of this thesis work using GPS equipment and a Brunton compass to measure strikes and dips, as well as obtaining hand samples to use for thin section work. Thin sections were used to obtain a clearer impression of the timing of events seen within the quarry, as well as to give insight into differences found in laminae containing bitumen fractures.

Regional Geology

On a regional scale, the geology in Southern Oklahoma has undergone a number of changes over time. From the Precambrian to the Cambrian, the region experienced a period of failed rifting which led to the Southern Oklahoma Aulacogen (Keller, 1983; McConnell,1990). During the Middle Cambrian, the Aulacogen continued into a period of igneous activity, evidenced by granites and rhyolites found throughout the region

(Gilbert, 1983). This was followed by a period of thermal subsidence. Thermal equilibrium was reached by the end of the Ordovician (Garner, 1984). During the Carboniferous these extensional tectonics switched to compressional, creating fault zones and uplifts which sketched the image of Oklahoma's modern geologic provinces (McCullough, 2014). The periods of early extension created topographic lows which would later become an epicontinental sea (McCullough, 2014).

The Woodford Shale, the focus of this work, was deposited starting in the Late Devonian and into the Early Mississippian (Turner, 2016). It unconformably overlays the Hunton and is overlain itself by the Sycamore Limestone (McCullough, 2014; Turner, 2016). In some locations pockets of Misner Sandstone are deposited between the Hunton and the Woodford, being more common to the north (Turner, 2016). The Misner is interpreted to potentially be from an early stage of Woodford transgression (Turner, 2016; R. Slatt, personal communication, 2017).

The top of the Hunton shows evidence of karsting and erosion, which indicates that the Hunton was subaerially exposed prior to the deposition of the Woodford (Turner, 2016). Deposition of the Woodford began with the transgression of the Paleotethys due to eustatic sea level rise during the Late Devonian (Infante-Paez, 2015). This transgression continued through to the end of the deposition of the Middle Woodford, when the Paleotethys began to regress (Turner, 2016).

The thickness of the Woodford is determined by paleotopography, thinning landward and thickening distally (Turner, 2016). In addition, the thickness of the Woodford tends to have an inverse relationship with the thickness of the Hunton. This has been interpreted as a paleo-incised valley-karst system where the thickness change

is caused by preferential backfilling of the valley during the transgression of the Paleotethys (McCullough, 2014).

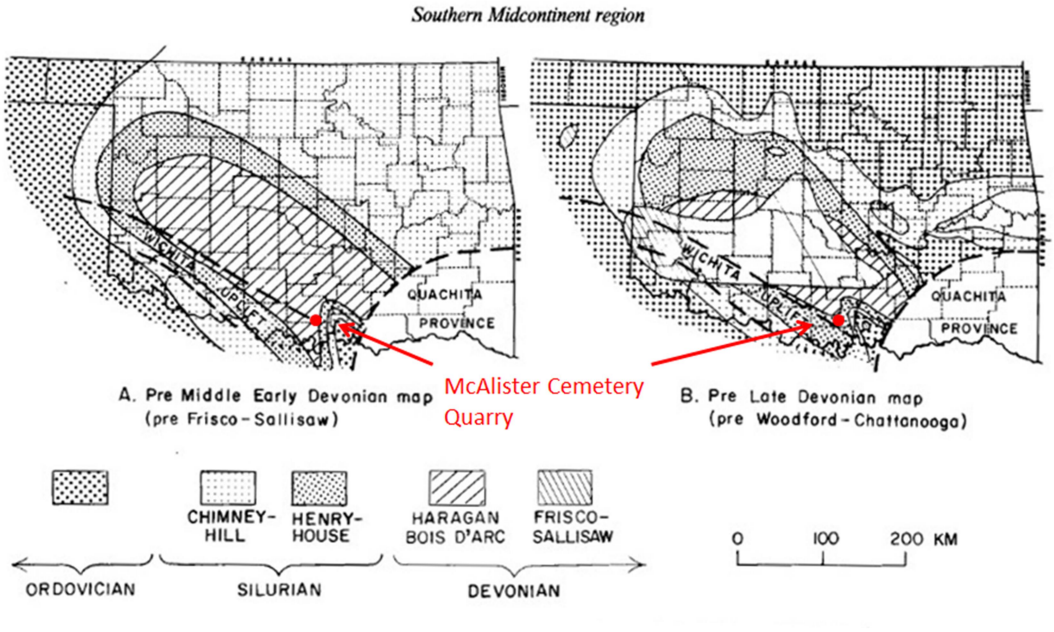

Figure 4 Paleogeologic maps of Oklahoma Basin following major epeirogenic uplifts (Figure credit: modified from Johnson et. al, 1989).

Local Geology

On a local scale, the McAlister Cemetery Quarry (Figure 5) is located in T. 5 S, R. 1 E, Section 36 in Carter County. This is in the Criner Hills, which are found between the Marietta and Ardmore Basins as shown in Figure 6. The Criner Hills are composed of three segments: the Criner Anticline, the Rock Crossing Anticline, and the Overlook Anticline. The quarry is located on a limb of the Rock Crossing anticline.

Figure 5 Satellite Image of McAlister Cemetery Quarry noting locations of Figures 7 through 15 and 18 through 20. Included in black are informal member contacts and structural features within the quarry (Figure credit Google, 2014).

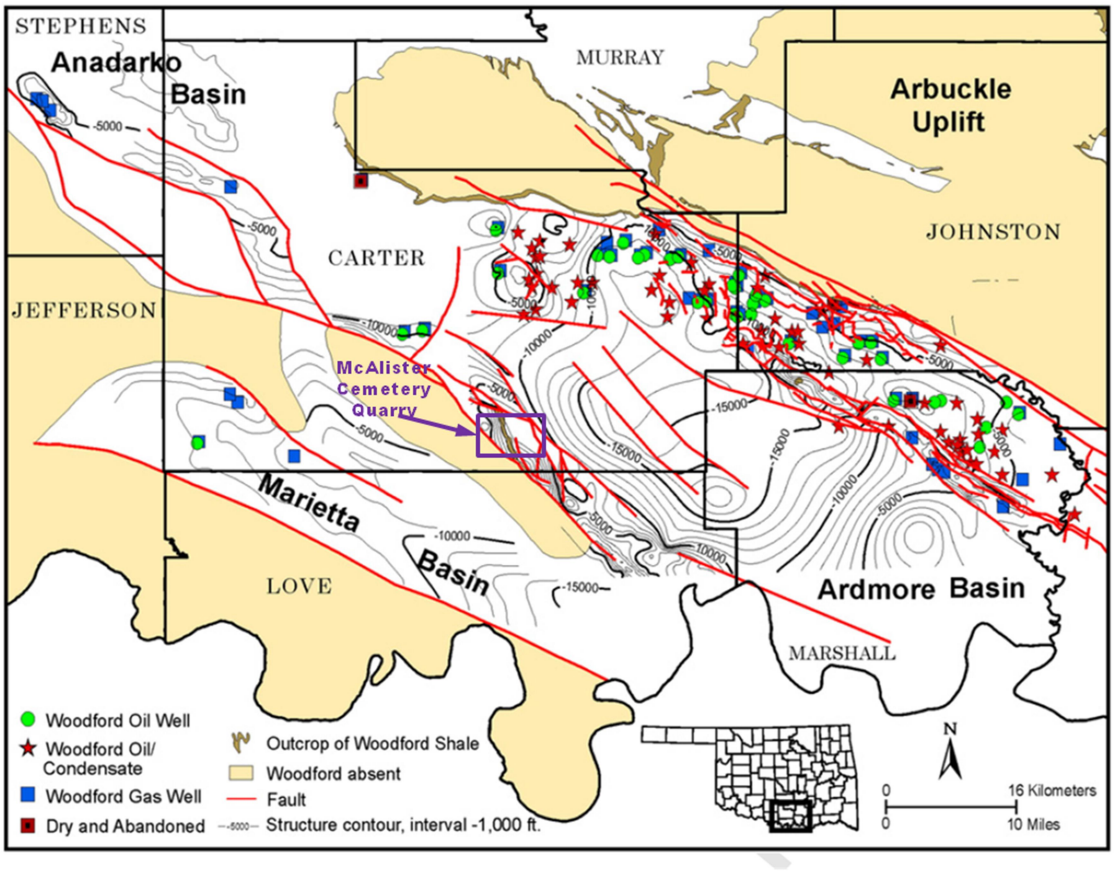

Figure 6 A map showing the location of the McAlister Cemetery Quarry. (Figure credit Cardott, 2012).

The quarry contains structural features trending NW-SE that are potentially folds or faults as addressed later. These features can be found on the North and East Walls within the quarry, seen in Figures 7 and 8. A set of mounds are situated in the center of the quarry, which give good exposures of the Middle Woodford (Figure 9). A layer of bitumen-filled fractures can be seen on the westernmost of these mounds. As survey work continued, more exposures of bitumen-filled fractures were found, however these were always constrained to the Middle Woodford.

Ongoing work by Ghosh indicates that there are five sets of these fractures determined by their size, orientation, and how much bitumen they contain (Figure 10). He has labelled these fractures in order of their occurrence relative to one another, such that fracture set 1 is the oldest and fracture set 4 is the most recent. The first set (1) contains thick sheets of bitumen with strikes trending east northeast, while the second set (2) contains thin sheets of bitumen with strikes trending northeast. These sets tend to crosscut each other. The third set of fractures (3S) are smaller, still containing bitumen, and tend to truncate at the second set of fractures. The fourth set of fractures (3P) are cement and bitumen free, and trend east, parallel to bedding. The fifth set of fractures (4) is the least common, may occasionally contain bitumen, and truncates at the first set of fractures (Ghosh, 2016).

Figure 7 North Wall Viewed from the South. The fold on this wall is subtle, and can be found to the left side of the image. This wall presents a very clear section of the Middle Woodford, and was thoroughly investigated by Serna-Bernal for her thesis (Serna-Bernal, 2013; Ekwunife, 2017).

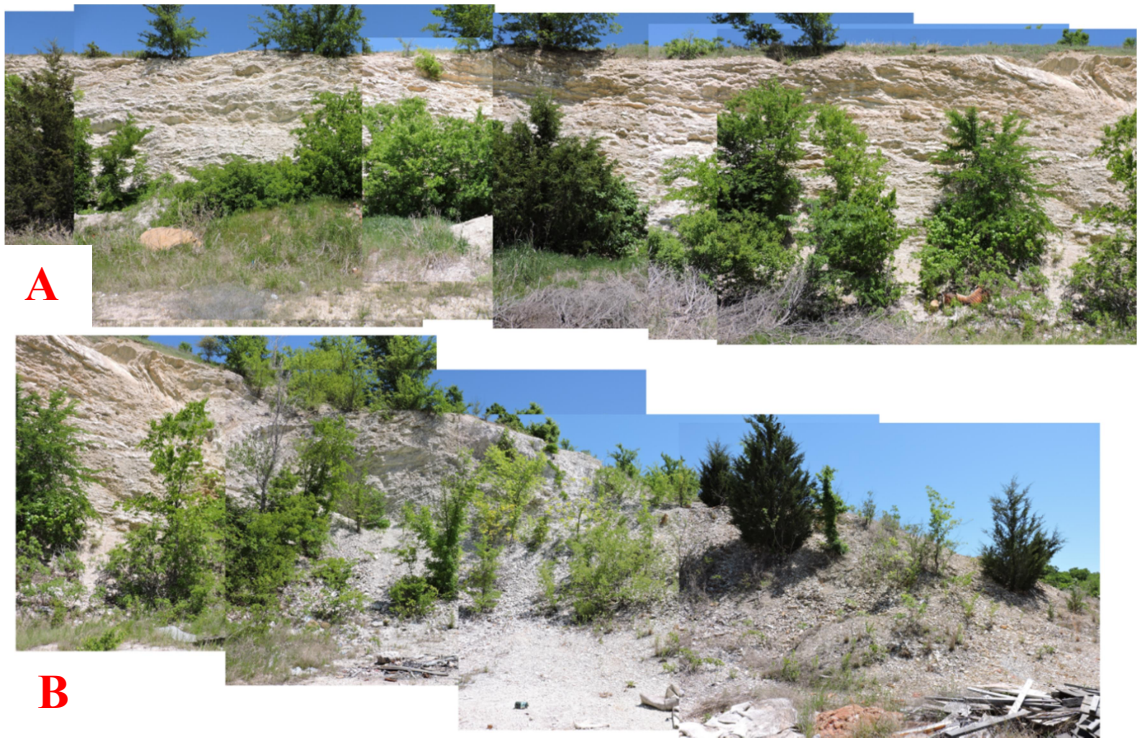

Figure 8 East Wall, A trends North-South, B trends east-west. This wall is composed entirely of the Upper Woodford.

Figure 9 Central Mounds as viewed from the Eastern Wall in the top photo and from the base of the Northern Wall in the bottom photo.

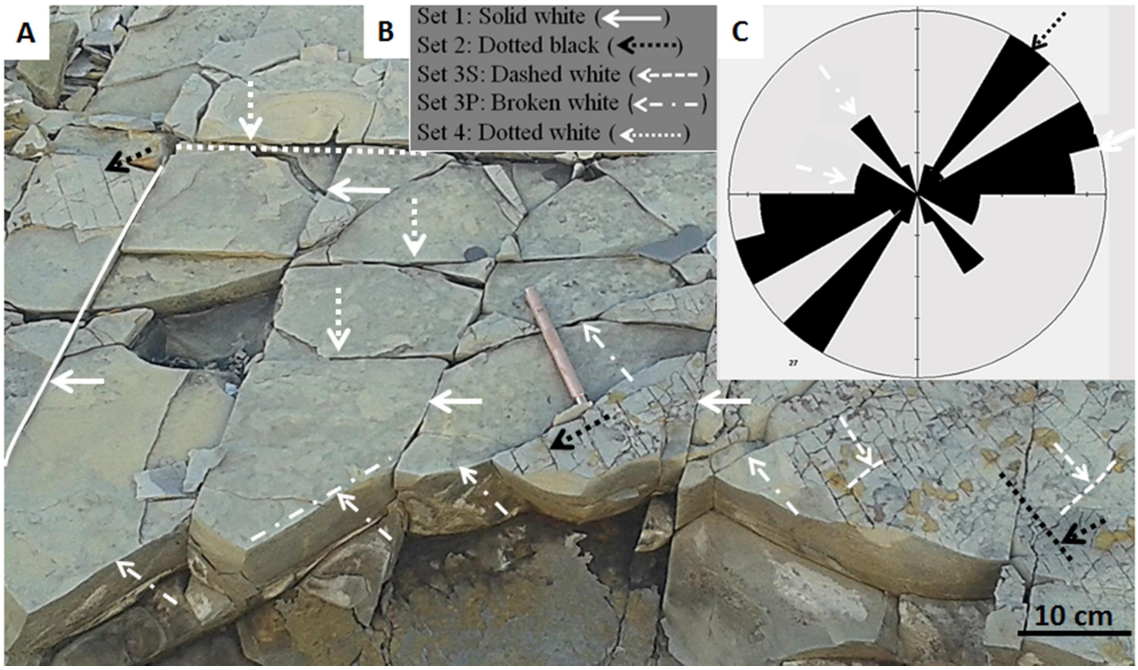

Figure 10 A. This image shows the various fractures sets as they appear outcropping on the Central Mounds. Fractures are labeled in order of relative age, with Set 1 being the oldest and Set 4 the most recent. B. This figure shows each fracture set as defined by Ghosh. Black arrows indicate that the fracture set contains bitumen while white arrows indicate the fracture set contains no infill. C. A rose diagram showing the strikes of the fracture sets. (Modified from Ghosh, 2016).

Figure 11 Large Concretions, located above the North Wall. These three concretions are from the Upper Woodford and were used as markers for control measurements during GPS acquisition.

Geologic Field Methods and Observations

As part of continuing work in the McAlister Cemetery Quarry by the Institute for Reservoir Characterization, a geologic map integrating various field measurements of the quarry was created. This includes structural features such as fractures, faults, folds, and a complete stratigraphic section of the Woodford Shale. In addition to GPS data acquisition, strike and dip measurements were acquired whenever possible with reliable accuracy. Thin sections were taken to assess continuity between features in the quarry, and to determine fracturing and bitumen presence on the microscopic scale.

Work in the quarry began with a general survey to look for any visual clues to determine the existence of faults and folds. In the northern part of the quarry, the Middle Woodford is highly fissile and shows jointing, but no major signs of faulting or folding. The Middle Woodford tends to be more competent in the center of the quarry

where the mounds are, however due to quarrying activity these mounds have been largely covered with debris. This initially threw doubt on the possibility that these features were *in situ*, though later work showed that strikes and dips in this area are consistent enough that it was determined that they were undisturbed. This was with the exception of the southern tip of the mounds, which can be seen on the map as a circular portion where the gravel roads intersect. The strikes and dips of the rock here are too irregular to be deemed *in situ*. Exposed rock surfaces in the central mounds show numerous examples of bitumen-filled fractures (Figure 12).

Figure 12 Bitumen-filled fractures located on the east facing side of the Central Mounds.

Figure 13 Multiple views of the feature on the Eastern Wall showing it to be an overturned fold. Red lines represent layers of bedding while the yellow line shows how the axial plane crosses through the bedding plane. From the position the bottom photograph was taken, an azimuthal trend was measured at 133 degrees.

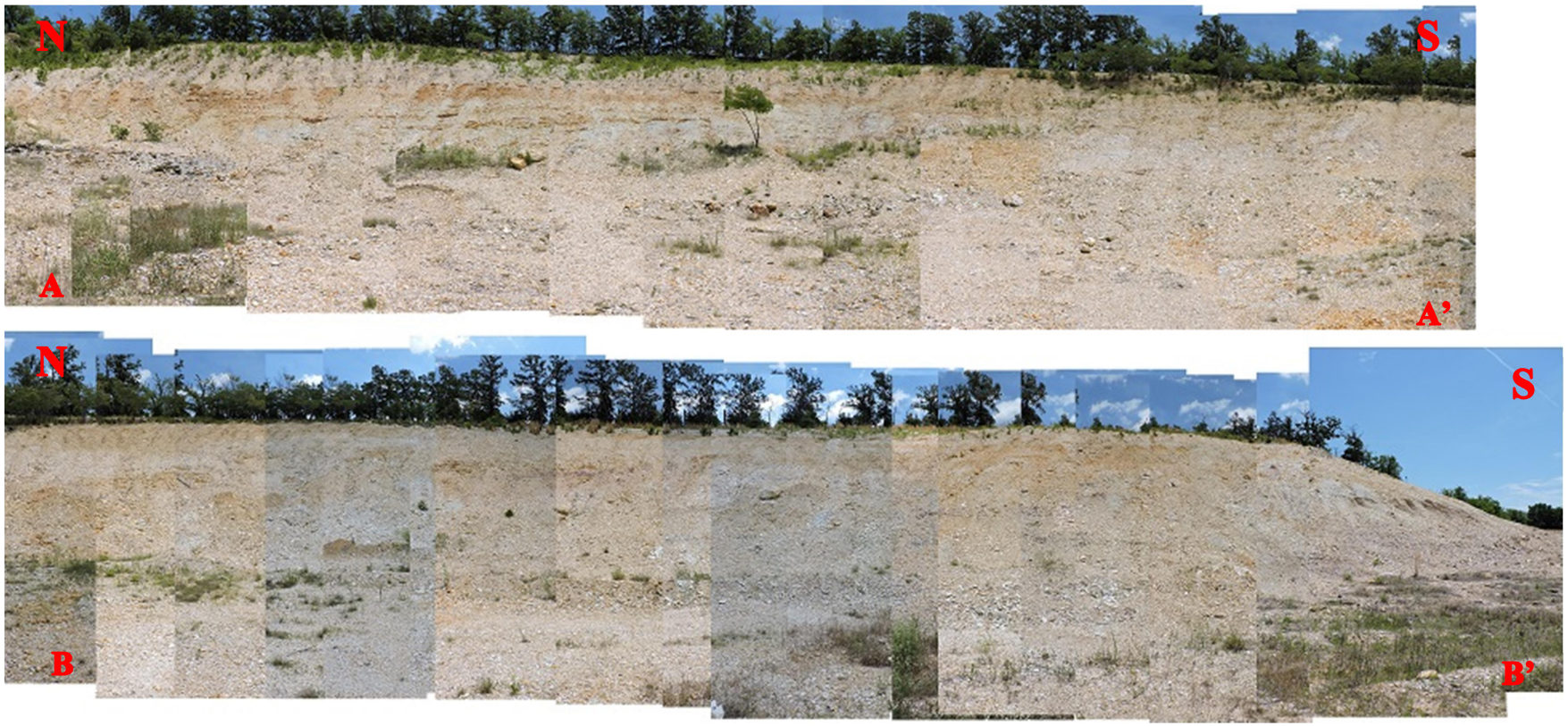

Figure 14 South Wall, trends north-south. Top and bottom photos connect at A' and B to show the entirety of the wall. The majority of this wall is composed of Upper Woodford, and upon careful observation, small scale faulting can be seen in the offset of some of the beds.

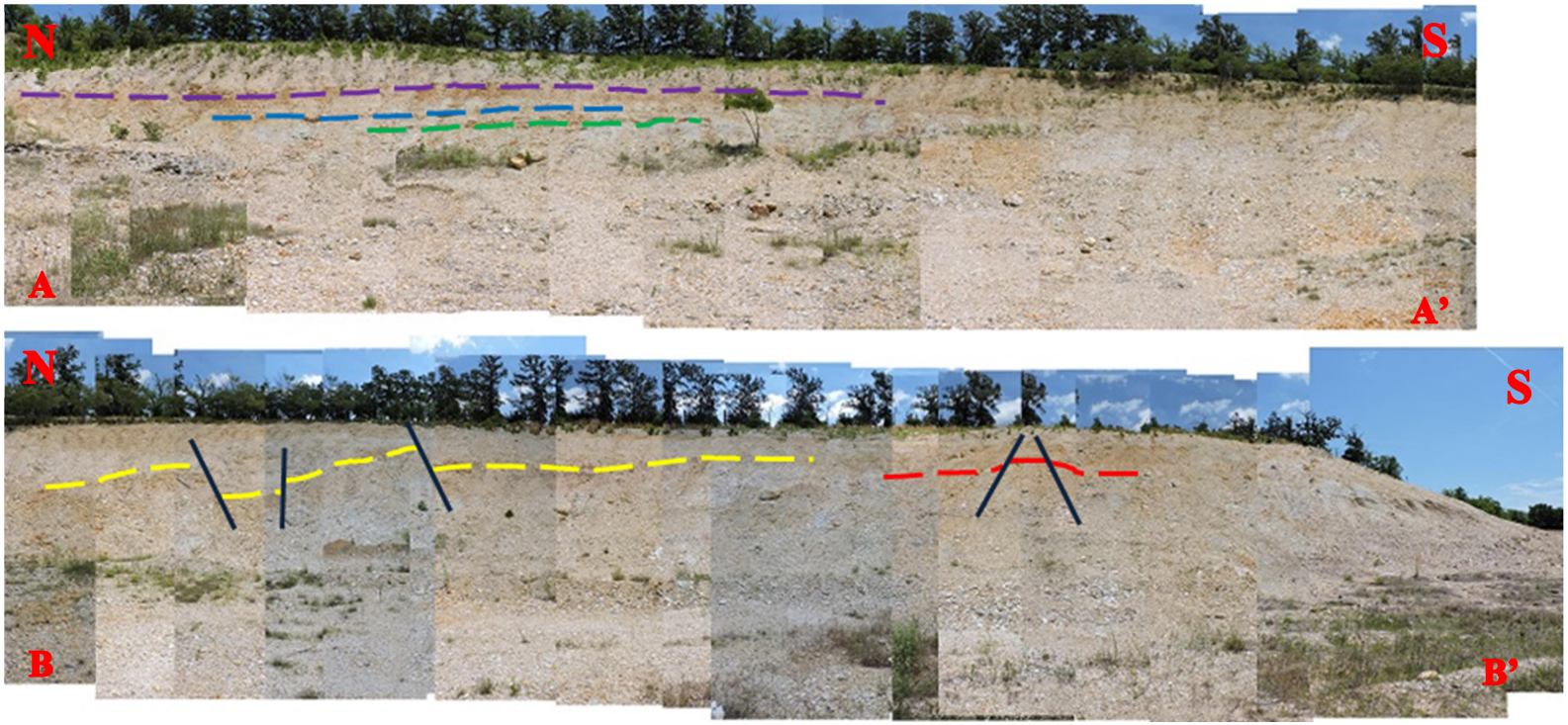

Figure 15 South Wall, trends north-south. Top and bottom photos connect at A' and B to show the entirety of the wall. The majority of this wall is composed of Upper Woodford, and upon careful observation, small scale faulting can be seen in the offset of some of the beds, which have been marked. Figure A to A' bedding remains largely parallel, as can be seen with the purple, green, and blue dashed lines. However, in figure B to B' the faulting can be seen, as marked by the yellow and red dashed lines.

There has been internal discussion amongst IRC members regarding the nature of a structure seen near the top of the wall on the eastern side of the quarry, too high to be easily measured. High resolution images (Figure 13) of this structure were taken when the sun was directly hitting the wall, in order to ensure that no shadows could obscure or distort the structure. In the southern portion of the quarry, bedding has been even more disrupted by past quarrying activity; however some intact rock can be seen outcropping in a wall running along the eastern side of the quarry. Shale here seems to show faulting as individual laminae can be traced across the wall before dropping to a lower elevation relative to the base of the wall. Photos of this phenomenon have likewise been taken and analyzed (Figures 14 and 15).

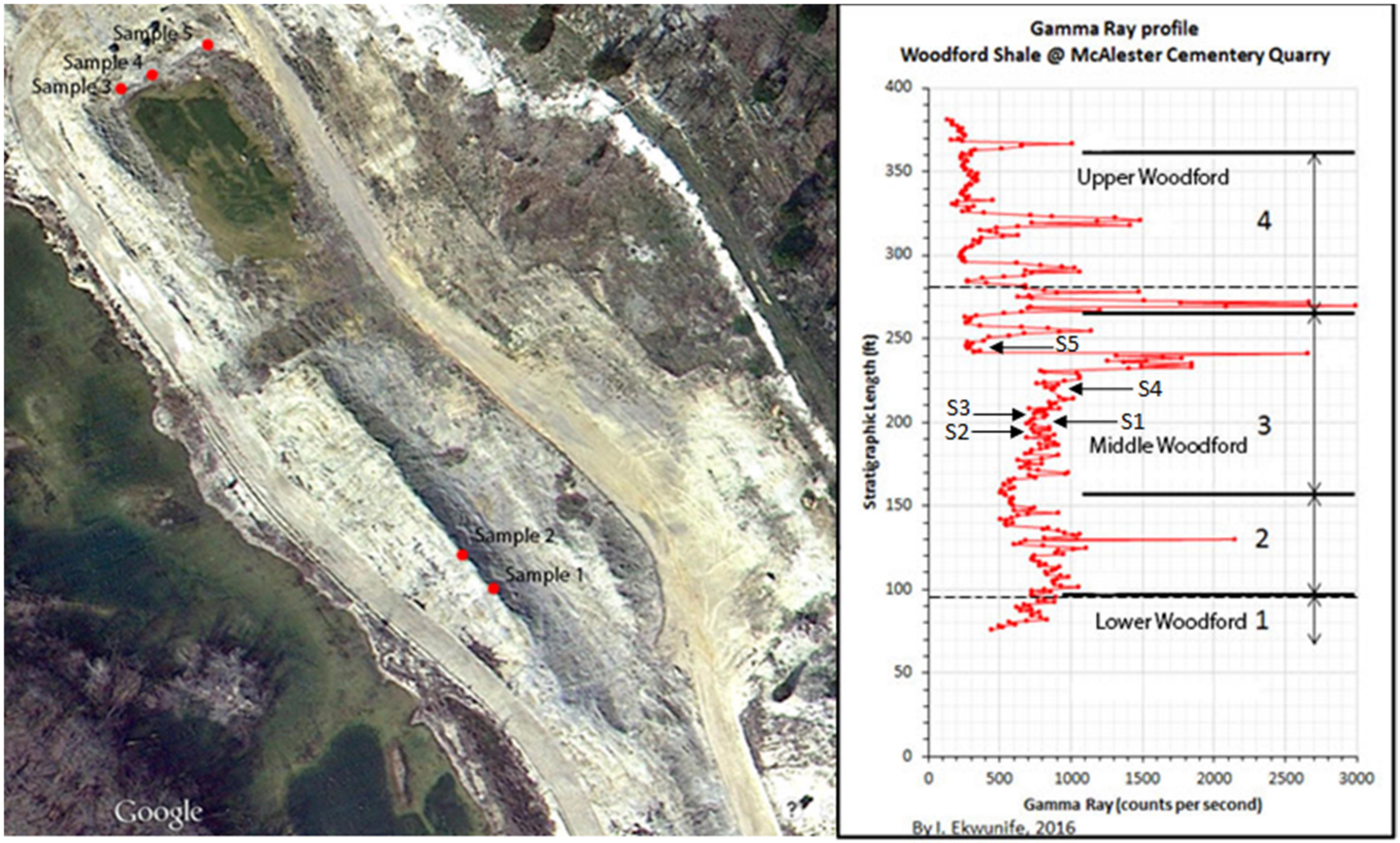

Figure 16 Sampling Locations. Samples 1 and 2 were taken from the Central Mounds, and Samples 3-5 were taken from the North Wall. S1 through S5 refers to samples 1 through 5 as they are located on a gamma ray log of the Woodford within the quarry. Figure modified from Ekwunife, 2016.

Hand samples were taken from five sites throughout the center of the quarry (Figure 16), with a focus on outcrops of shale containing bitumen-filled fractures. These hand samples were used to create thin sections which were examined for any changes in composition which might have allowed for the creation of the fractures. Initially, there appeared to be a correlation between where the fractures appeared and how clean or fine grained the shale was. This did not hold true for all of the samples.

Mapping began by gathering GPS data throughout the quarry while taking measurements of strike and dip. GPS data was acquired using daily measured control points which were then tied back to a known base station in Ardmore, Oklahoma. This correction calculation was then applied to data gathered in the field. In total around 75 measurements were taken throughout the quarry. The GPS data were then used to create a topographic map of the quarry which was overlain by a satellite image. Strikes and dips were plotted on top of this combination image, in addition to points of interest including the North Wall, East Wall, mounds, and lakes (Figure 17).

Initially, the contact between the Middle and Upper Woodford was plotted at the white marker bed mentioned earlier using ground observations, GPS measurements, and strike and dip data. This data, along with stratigraphic thickness measurements of 95 feet in the Lower Woodford, 133 feet in the Middle Woodford, and 144 feet in the Upper Woodford (Serna-Bernal, 2013) were used to calculate the surface thickness of each member of the Woodford using basic trigonometric calculations. To plot the folds of the Eastern wall, the axis of the exposed syncline was measured at 133˚ by sighting with a Brunton compass. When this measurement was used for the corresponding anticline, the anticline matched up with another feature of the quarry found on the North

Wall. On the south side of the East Wall we can see the transition between an anticline and syncline, as shown in Figure 20.

During the course of making the map, the boundary between the Middle and Upper Woodford was redefined to be the lowest point at which phosphate nodules could be found in the quarry. Field observations from the quarry placed the new boundary in its current position, and the lowest locations at which phosphate nodules were found has been marked on the map in yellow. Other boundaries were kept in place as they still corresponded to the definitions provided by Serna-Bernal (Serna-Bernal, 2013). Bed thicknesses of the Upper, Middle, and Lower Woodford are now 92 feet, 185 feet, and 95 feet respectively.

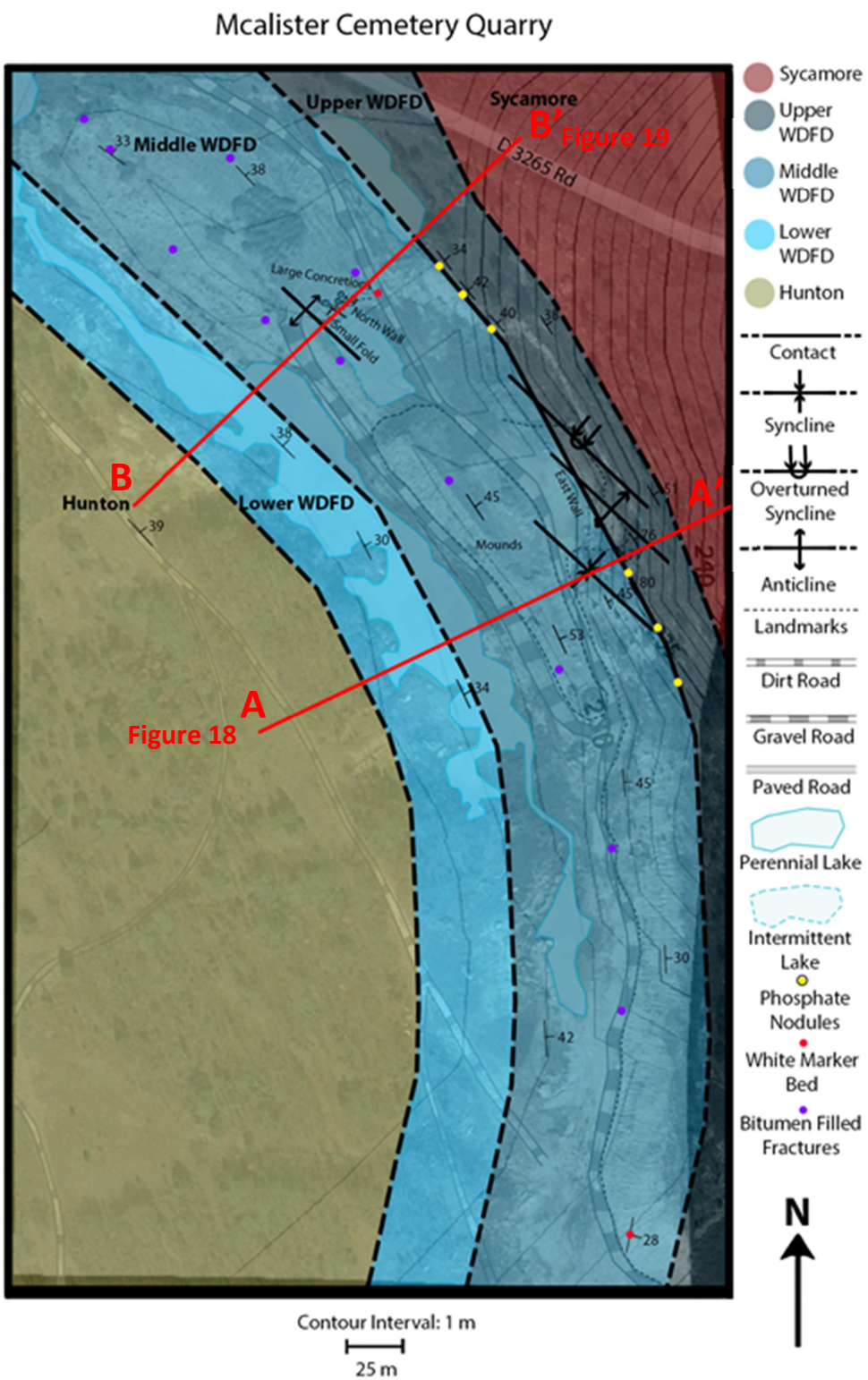

Figure 17 Geologic Map of McAlister Cemetary Quarry layered over Google Earth 2014 image.

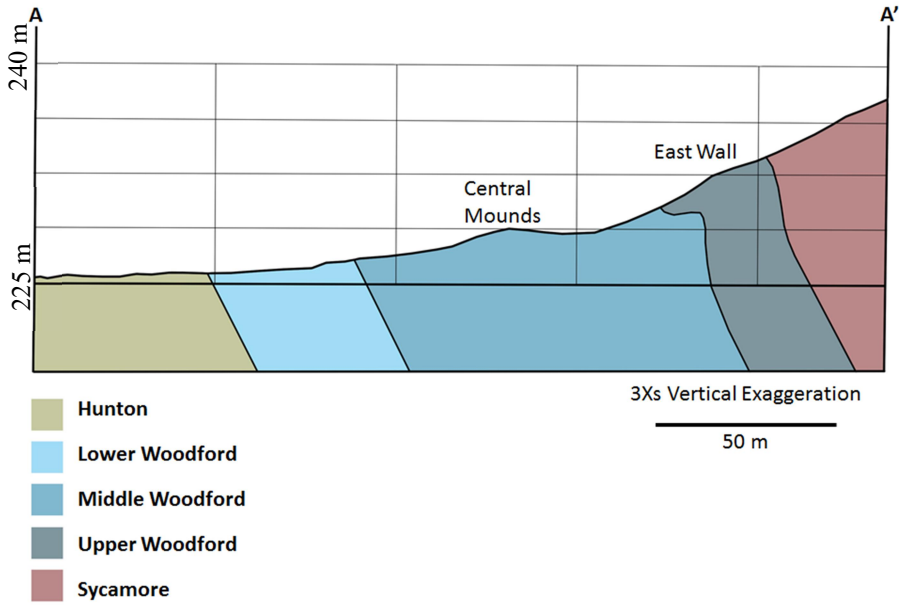

Figure 18 Cross Section A-A' with a 3Xs vertical exaggeration. Beds to the west dip 34 ºE. Between the Middle and Upper Woodford and the Upper Woodford and Sycamore, beds range in dip from 51ºE to 80ºE. Dips shown in figure are exaggerated.

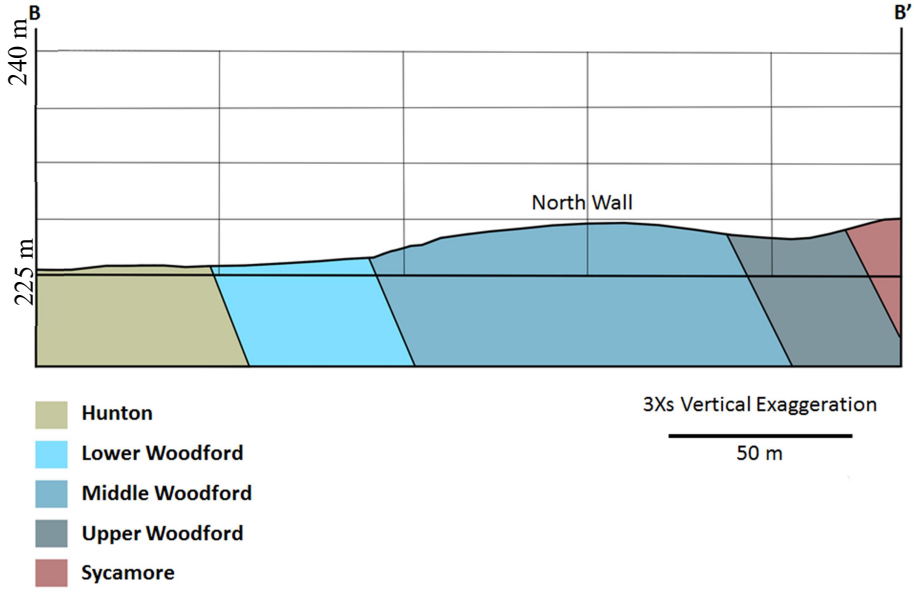

Figure 19 Cross Section B-B' with a 3Xs vertical exaggeration. Beds near the Hunton/Lower Woordford contact dip 39ºE and 38ºE on average from the Lower Woodford through the Sycamore. Dips shown in figure are exaggerated.

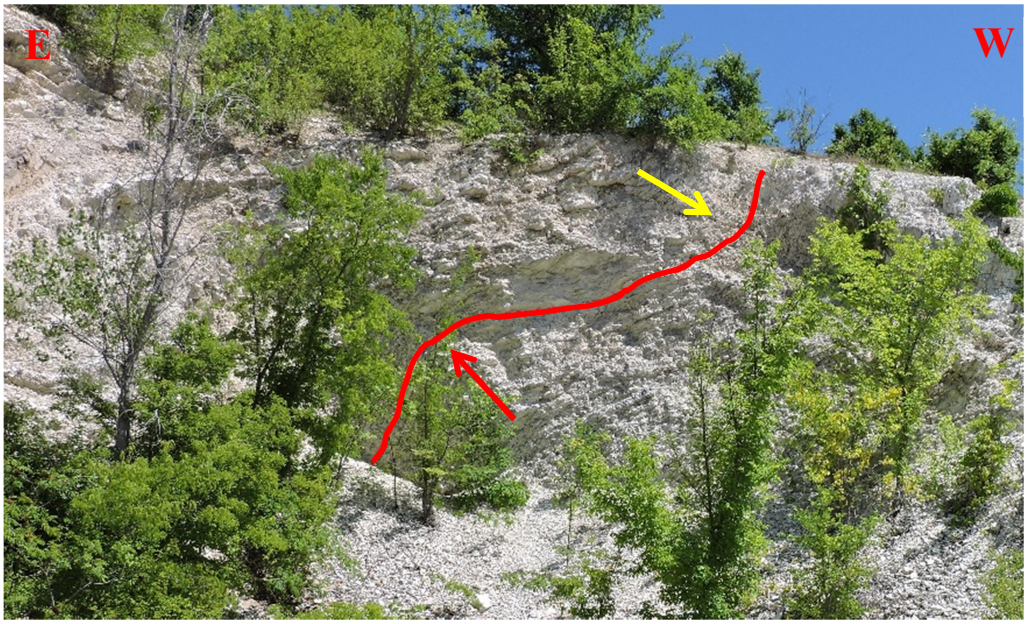

Figure 20 Feature on the South Side of the East Wall showing transition from anticline (red arrow) to syncline (yellow arrow). Fold axis was measured at 133º, beds dip at 51º on the eastern side of the image, and 77º on the western side.

Thin Section Analysis

Five hand samples were taken from the Middle Woodford in the center of the quarry (Figure 16). Two of these samples were taken from the Central Mounds while three were taken from the Northern Wall. This was in order to determine if bedding was continuous from the Central Mounds to the Northern Wall. Samples were selected from laminae containing bitumen-filled fractures and marked in the field to denote stratigraphic top from bottom. Any loose sections of the hand samples were secured with epoxy.

Grain size was examined under 10X magnification. If the sample was well sorted, then an average grain size was calculated by measuring multiple grains and taking the average. In the case of poorly sorted samples, an average was not considered

to be representative and so a range was given instead. Each sample was divided into thirds from top to bottom for these measurements.

According to Serna-Bernal, the Middle Woodford contains three main facies: laminated siliceous shale, laminated siliceous siltstone, and laminated finely crystalline dolomite. The Middle Woodford also contains quartz and dolomite rich intervals which are found in different forms. These different forms for quartz include: detrital quartz, authigenic quartz filling tasmanites, and diagenic quartz in the form of recrystallized radiolarians. Dolomite comes in the form of anhedral crystals (Serna-Bernal, 2013).

Sample 1 contains graded bedding, and fines upwards. At the base of the sample, grain size ranges from 5 μm to 80 μm, with an average of 40 μm (Figure 21). In the middle, grain size ranges from 5 μm to 60 μm, with an average of about 30 μm (Figure 22). At the top, grain size ranges from 5 μm to 30 μm, with an average of about 20 μm (Figure 23). Fractures occur in the finer grained and cleaner portion of this sample. This sample is also laminated, where the darker laminations are clay rich and the lighter laminations are radiolarian rich. Radiolarians appear to be either recrystallized or fractured.

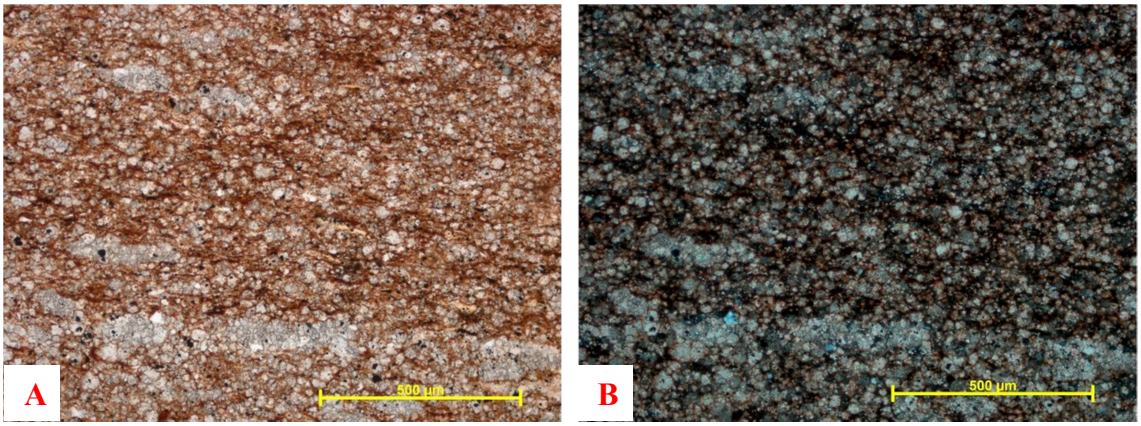

Figure 21 Base of Sample 1, 10 X magnification. Image A shows the sample in plane polarization while image B shows it in cross polarization. Grains range in size from 5 µm to 80 µm, with an average of 40 µm.

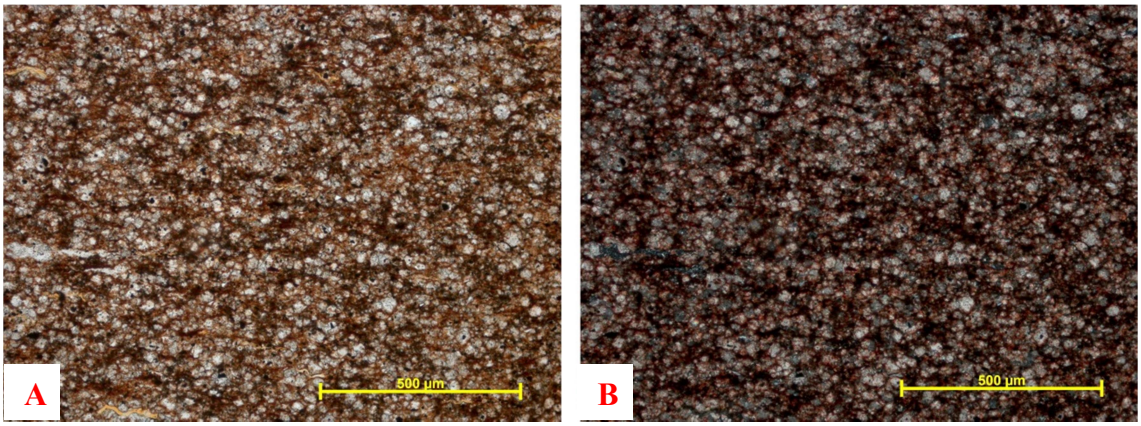

Figure 22 Middle of Sample 1, 10 X magnification. Image A shows the sample in plane polarization while image B shows it in cross polarization. Grains range in size from 5 µm to 60 µm, with an average of 30 µm.

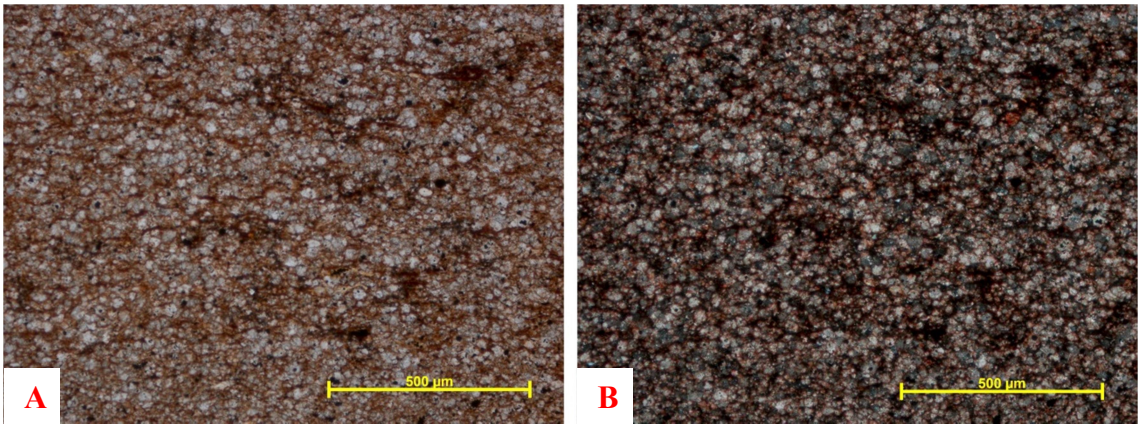

Figure 23 Top of Sample 1, 10 X magnification. Image A shows the sample in plane polarization while image B shows it in cross polarization. Grains range in size from 5 µm to 40 µm, with an average of 20 µm.

Sample 2 does not contain any apparent natural fractures. Visible fractures are open, indicating that they were created at the time of the sample's acquisition. Grain size varies from top to bottom. The larger grains at the base (Figure 24) are oblong and as such, grains at the base range from 5 µm to 50 µm by 300 µm, with an average of around 20 µm. In the middle grains range from 5 µm to 60 µm, with an average of around 20 µm (Figure 25) while the grains at the top (Figure 26) range from 5 µm to 30 µm, with an average of around 10 µm showing again that the bedding fines upwards. The base is more poorly sorted. Overall many of the grains in this sample appear oblong, and the sample itself displays distinct lamination, with the grains aligned horizontally.

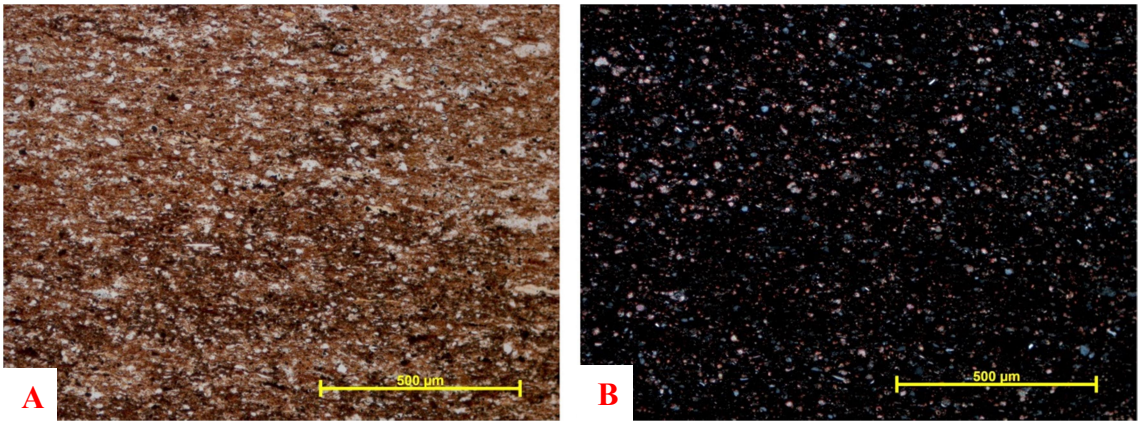

Figure 24 Base of Sample 2, 10 X magnification. Image A shows the sample in plane polarization while image B shows it in cross polarization. Grains range in size from 5 µm to 5 µm by 300 µm, with an average of 20 µm.

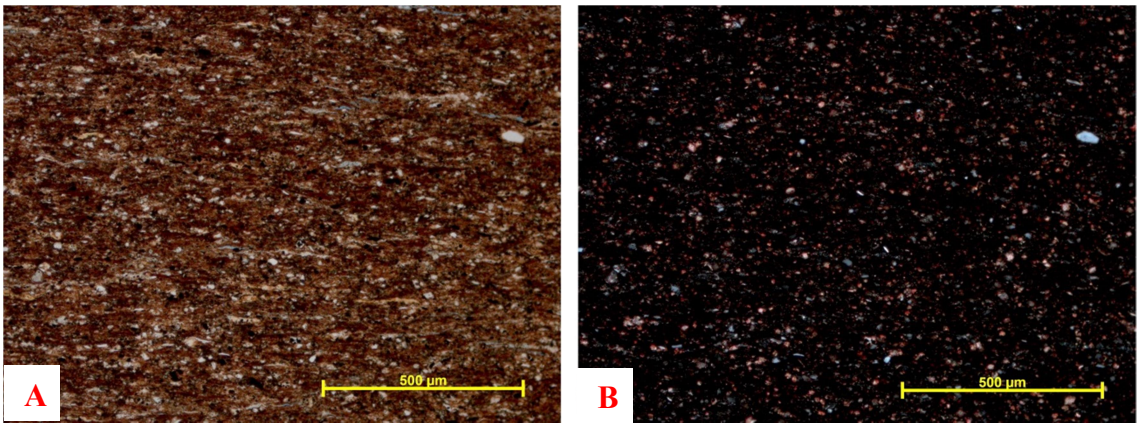

Figure 25 Middle of Sample 2, 10 X magnification. Image A shows the sample in plane polarization while image B shows it in cross polarization. Grains range in size from 5 µm to 60 µm, with an average of 20 µm.

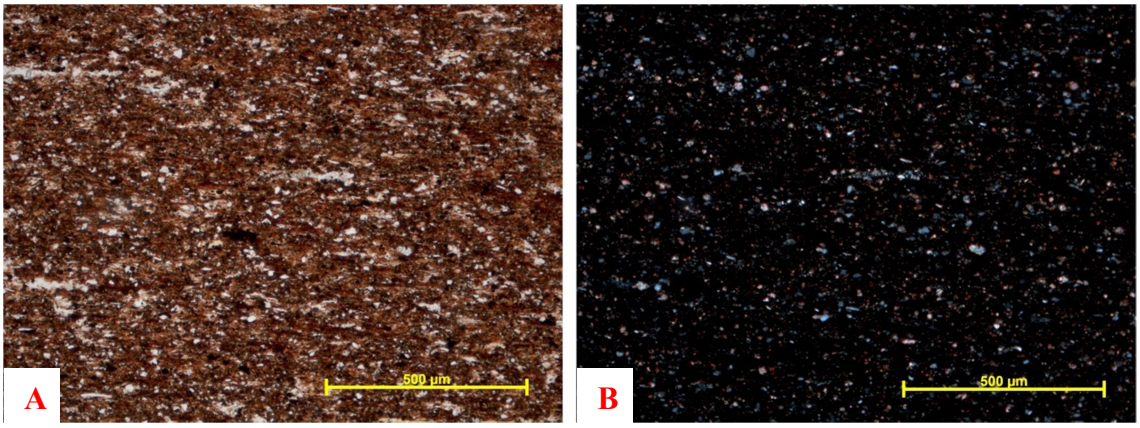

Figure 26 Top of Sample 2, 10 X magnification. Image A shows the sample in plane polarization while image B shows it in cross polarization. Grains range in size from 5 µm to 30 µm, with an average of 10 µm.

Sample 3 contains a large quantity of radiolarians and three sizable bitumen-filled fractures which are around 2 mm to 4 mm long which cut perpendicular to bedding. These fractures are found in the bottom and top of the sample, where the grains are poorly sorted and range in size from 5 µm to 180 µm (Figures 27 and 29). In the center the grains are also very poorly sorted, ranging in size from 5 µm to 250 µm (Figure 28).

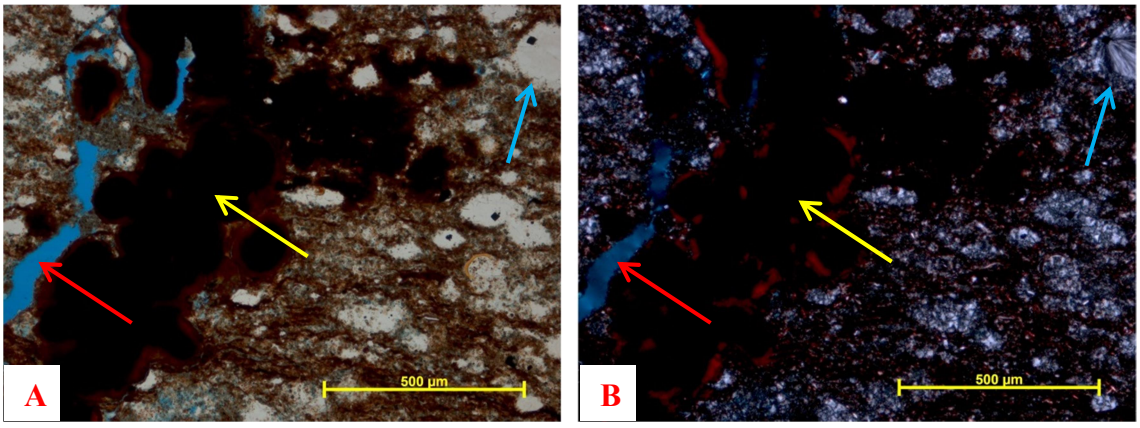

Figure 27 Bottom of Sample 3, 10 X magnification. Image A shows the sample in plane polarization while image B shows it in cross polarization. Grains are very poorly sorted and range in size from 5 µm to 180 µm. Yellow arrows indicate the bitumen infill of the fracture, blue arrows indicate examples of radiolarians, and red arrows indicate open spaces in the fractures which were likely acquired during sample acquisition.

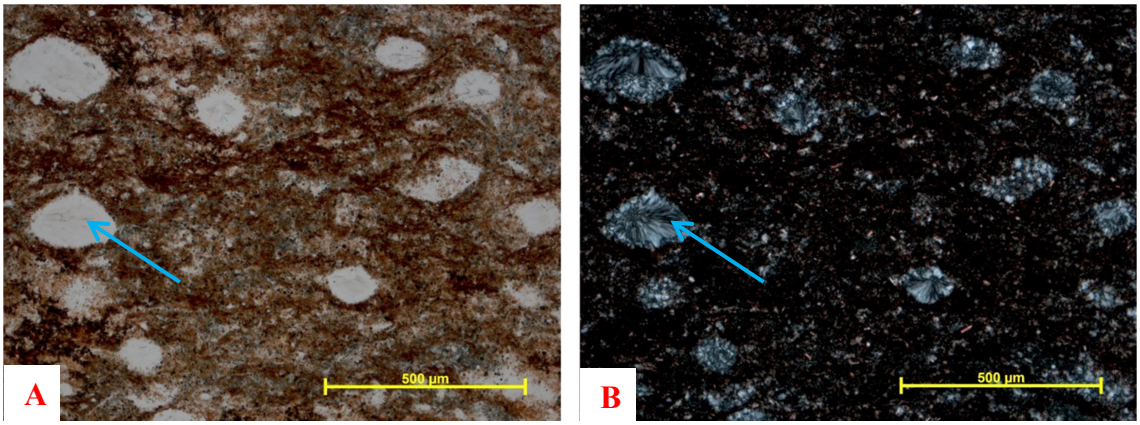

Figure 28 Middle of Sample 3, 10 X magnification. Image A shows the sample in plane polarization while image B shows it in cross polarization. Grains are very poorly sorted and range in size from 5 µm to 250 µm. Blue arrows indicate examples of radiolarians.

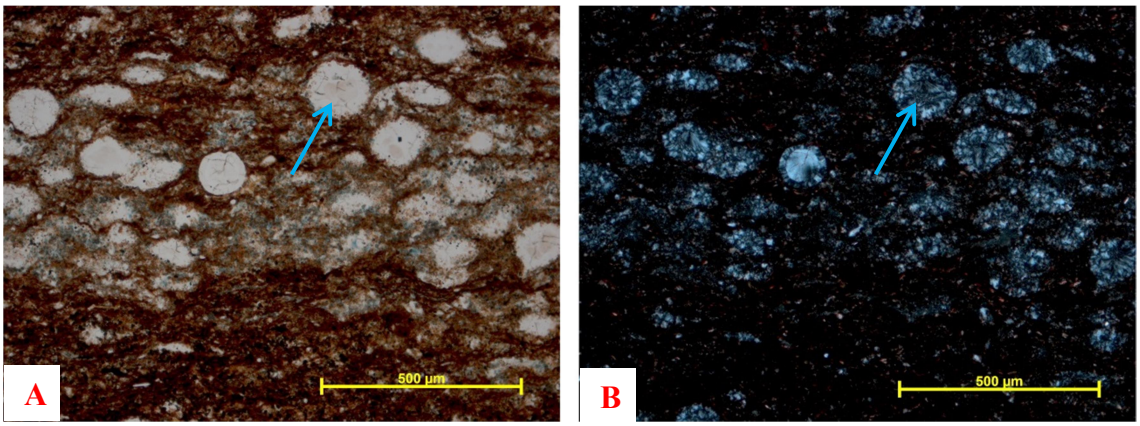

Figure 29 Top of Sample 3, 10 X magnification. Image A shows the sample in plane polarization while image B shows it in cross polarization. Grains are very poorly sorted and range in size from 5 µm to 180 µm. Blue arrows indicate examples of radiolarians.

Sample 4: Grain size throughout the sample averages around 10 µm to 30 µm wide and 1000 µm or greater in length, where the larger grains are oblong. The bottom of the sample is slightly coarser grained and more moderately sorted than the rest of the sample, with grains ranging in size from 10 µm to 40 µm, averaging around 20 µm (Figure 30).The center of the sample is medium grained and moderately sorted, with

grain sizes ranging from 5 µm to 50 µm, with an average of around 20 µm (Figure 31). The top of the sample is fine grained and well sorted, with grain sizes ranging from 5 µm to 20 µm, averaging around 10 µm (Figure 32). The top contains several fractures which are horizontal, following the direction of bedding, and oblique fractures cutting across bedding. The horizontal fractures are distributed without regard to grain size while the oblique fractures appear to be filled with bitumen. In addition, the bitumen-filled fractures appear to cut along planes of weakness within the calcite filled fractures. This suggests that the event which created the bitumen-filled fractures occurred after the event that created the calcite filled fractures.

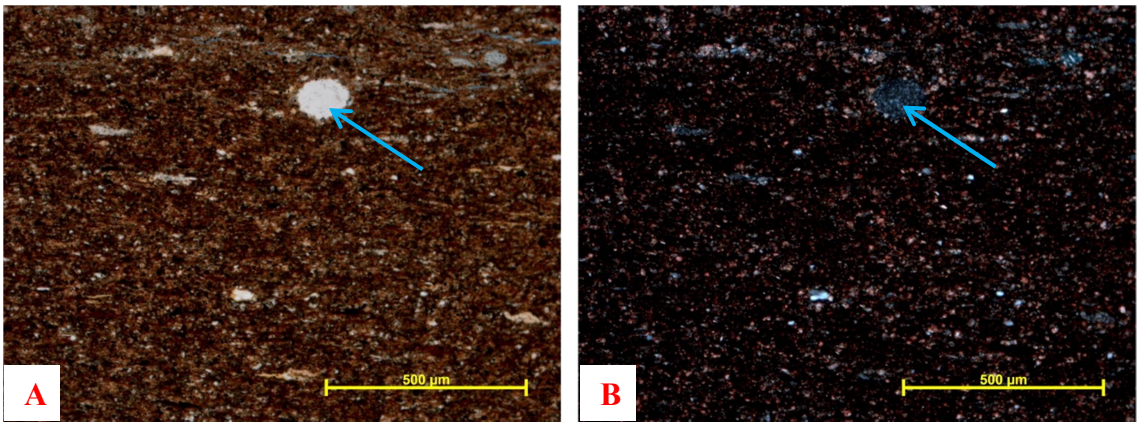

Figure 30 Bottom of Sample 4, 10 X magnification. Image A shows the sample in plane polarization while image B shows it in cross polarization. Grains are moderately sorted and range in size from 10 µm to 40 µm, with an average around 20 µm. Blue arrow indicates a radiolarian.

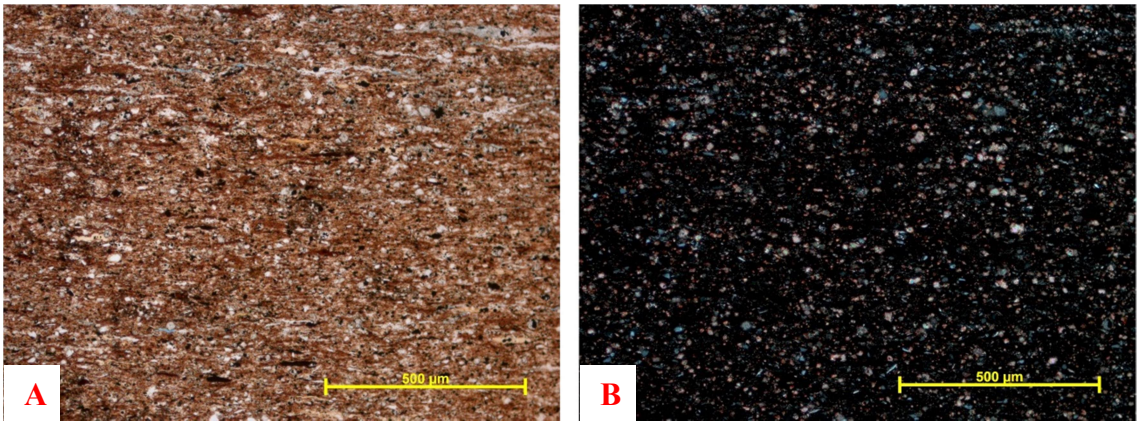

Figure 31 Middle of Sample 4, 10 X magnification. Image A shows the sample in plane polarization while image B shows it in cross polarization. Grains are moderately sorted and range in size from 5 µm to 50 µm, with an average around 20 µm.

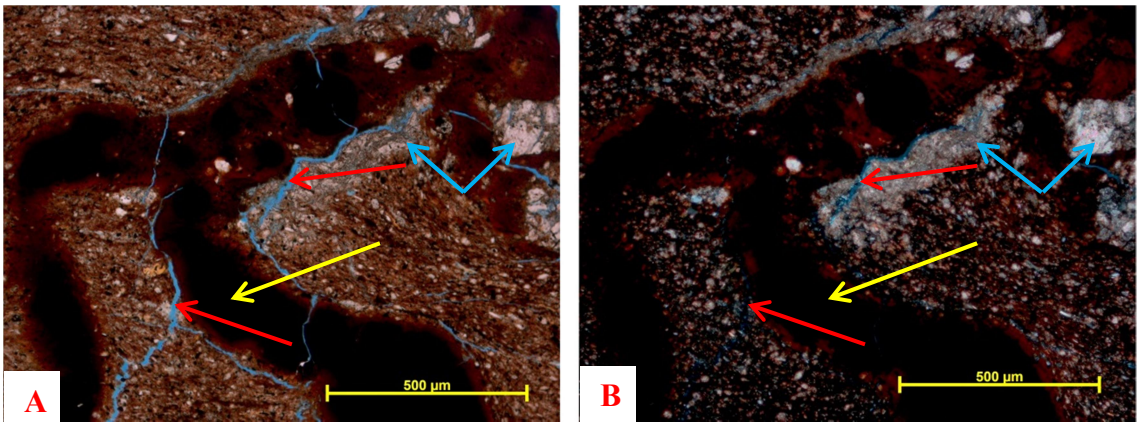

Figure 32 Top of Sample 4, 10 X magnification. Image A shows the sample in plane polarization while image B shows it in cross polarization. Grains are well sorted and range in size from 5 µm to 20 µm with an average around 10 µm. Yellow arrows indicate the bitumen infill of the fracture, and red arrows indicate open spaces in the fractures which were potentially acquired during sample acquisition. Blue arrows indicate calcite infill which has been cut along a plane of weakness by the bitumen infill.

Sample 5 contains fractures large enough to be seen without the aid of a microscope. These fractures are mostly bitumen filled, and often demonstrate an en echlon effect. In addition, sample 5 contains a large number of radiolaria. The radiolaria are found primarily within the center band of the hand sample, signaling a possible plankton bloom. Fractures range from .05 mm to 2 mm in width and can be several cm

long. Most often these fractures cut across bedding, but occasionally they follow parallel to bedding. Fractures tend to be larger and more common on the bottom of the sample. The base of the sample is poorly sorted, with grains ranging in size from 5 µm to 200 µm (Figure 33). The center of the sample is moderately to well sorted with grains ranging in size from 5 µm to 40 µm, averaging around 15 µm (Figure 34). At the top of the sample, grains tend to be moderately sorted, and range in size from 5 µm to 60 µm, averaging around 20 µm (Figure 35).

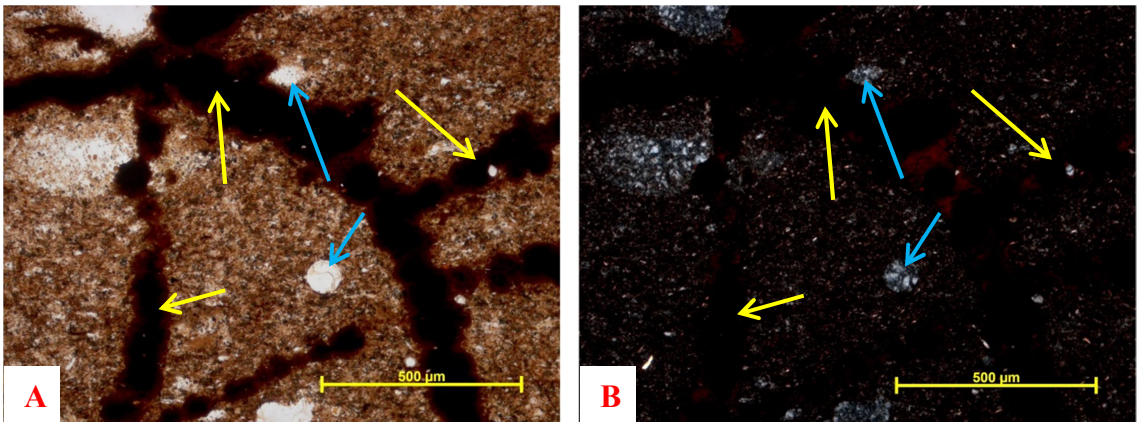

Figure 33 Bottom of Sample 5, 10 X magnification. Image A shows the sample in plane polarization while image B shows it in cross polarization. Grains are poorly sorted and range in size from 5 µm to 200 µm. Yellow arrows indicate the bitumen infill of the fracture, and blue arrows indicate examples of radiolarians.

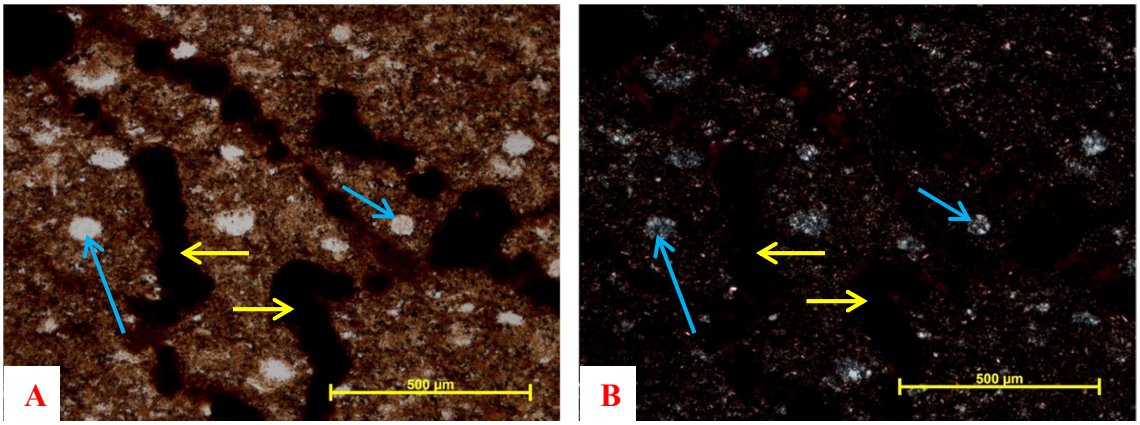

Figure 34 Middle of Sample 5, 10 X magnification. Image A shows the sample in plane polarization while image B shows it in cross polarization. Grains are moderately to well sorted and range in size from 5 µm to 40 µm with an average around 15 µm. Yellow arrows indicate the bitumen infill of the fracture, and blue arrows indicate examples of radiolarians.

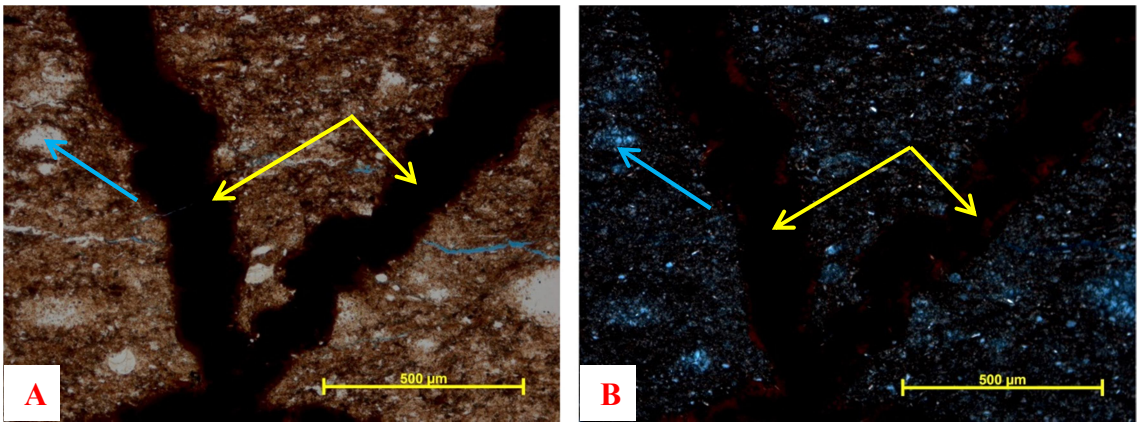

Figure 35 Top of Sample 5, 10 X magnification. Image A shows the sample in plane polarization while image B shows it in cross polarization. Grains are moderately sorted and range in size from 5 µm to 60 µm with an average around 20 µm. Yellow arrows indicate the bitumen infill of the fracture, and blue arrows indicate radiolarians.

All five samples showed at least a small amount of graded bedding, indicating sediment gravity flow and not suspension settling. Samples 1 and 2 from the Central Mounds most closely resembled sample 4, however after examining strike directions in the quarry it is unlikely that samples 1 and 2 correlate with sample 4. It is more likely

that they were created under similar circumstances, such that they closely resemble each other. Inflill of bitumen along previous planes of weakness was observed, giving evidence of relative age. This indicates that the event which created the bitumen filled fractures happened after the event which created the calcite filled fractures.

Conclusions

Several tasks were accomplished over the course of this thesis. The first was the creation of a geologic map of the McAlister Cemetery Quarry. This involved acquisition of new GPS data for the purpose of creating a topographic map, as well as accurately locating exposures of the Upper, Middle, and Lower Woodford. Locations of landmarks and other features of the quarry have been noted, including the locations of fractures within the strata.

Using the bed thicknesses provided by Andrea Serna-Bernal and Ifunanya Ekwunife, as well as strikes and dips taken from the quarry with strikes and dips provided by Sayantan Ghosh, surface bed thickness was calculated for the Upper, Middle, and Lower Woodford. When the boundary between the Middle and Upper Woodford was later redefined, these numbers were recalculated to approximately 92 feet for the Upper Woodford, 185 feet for the Middle Woodford, and 95 feet for the Lower Woodford.

During the course of gathering data for the geologic map, measurements of the mounds in the center of the quarry were taken to ascertain whether or not the mounds are *in situ* or are piles of debris from quarrying activities. Most of the mounds are *in situ*, as evidenced by having strikes that line up with the rest of the quarry. The only area found not to be *in situ* is the circular portion of the southernmost tip of the mounds,

which can be seen on the map near the intersection of the gravel roads. Despite man made disturbances in the quarry, the presence of fractures and structural features clearly indicate naturally occurring geologic movement.

Faulting and folding within the quarry was investigated. In the northern part of the quarry, the Middle Woodford is highly fissile and shows jointing, but no major signs of faulting or folding. Beds strike at 133º and dipped 38ºE on average. What structures are currently visible in the quarry have been documented, and seem to be restricted largely to the middle of the quarry; however more work will have to be done in the future to accurately measure these features. In the center of the quarry, beds strike at 155º and change dip due to folding found on the Eastern Wall. However the western side of the quarry dips 34º on average in this section. More accurate measures of the features on the Eastern Wall would involve obtaining a core sample at the fault on the North Wall, and the anticline on the East Wall.

Finally, thin sections were taken from samples from the Middle Woodford and analyzed for a mineralogical evaluation and to confirm the hypothesis that the mounds are indeed *in situ*. Thin sections displayed fractures occasionally infilled with bitumen and calcite. In at least one instance, the bitumen infill was observed cutting through a calcite filled fracture while taking advantage of a previous plane of weakness, indicating that the event which created the bitumen-filled fractures happened after the event which created the calcite-filled fractures. In addition, all five samples displayed graded bedding, indicating flow and not suspension settling.

References

"Ardmore, Oklahoma." Map. *Google Maps.* Google, 9 January 2014. Web. 9 January 2014.

Badra, H., 2011, Field characterization and analog modeling of natural fractures in the Woodford Shale, southeast Oklahoma: M.S. thesis, University of Oklahoma, Norman, OK, 78p.

Cardott, B. J., 2012, Thermal maturity of Woodford Shale gas and oil plays, Oklahoma, USA, International Journal of Coal Geology, p. 1-13. doi:10.1016/j.coal.2012.06.004.

Chain, A., 2012, Stratigraphy and Composition of the Woodford Shale in Depositionally Updip and Downdip Wells, Anadarko Basin, Oklahoma: M.S. thesis, University of Oklahoma, Norman, OK, 141p.

Ekwunife, I. Personal interview. 20 Nov. 2016.

Ellison, S.P. 1950. *Subsurface Woodford Black Shale, West Texas and Southeast New Mexico*, Texas Bureau of Economic Geology Report of Investigations, **7**, 22pp.

Garner, David L., and Donald L. Turcotte. "The Thermal and Mechanical Evolution of the Anadarko Basin." *Tectonophysics* 107 (1984): 1-24.

Ghosh, S. Personal interview. 17 Nov. 2016.

Gilbert, M C. "Timing and Chemistry of Igneous Events Associated with the Southern Oklahoma Aulacogen." *Tectonophysics* 94 (1983): 439-55.

Gupta, N., 2012, Multi-Scale Characterization of the Woodford Shale in West-Central Oklahoma: From Scanning Electron Microscope to 3D Seismic: Ph.D. dissertation, University of Oklahoma, Norman, OK, 148 p.

Infante-Paez, L. 2015, Seismically-Determined Distribution of Total Organic Carbon (TOC) in the Woodford Shale Through Integrated Reservoir Characterization, Payne County, Oklahoma: M.S. thesis, University of Oklahoma, Norman, OK, 79p.

Johnson, K.S., Amsden, T.W., Denison, R.E., Dutton, S.P., Goldstein, A.G., Rascoe Jr. B., Sutherland, P.K., and Thompson, D. M., 1989, Geology of the Southern Midcontinent. Oklahoma Geological Survey Special Publication 89-2, 1-53.

Keller, G R., E G. Lidiak, W J. Hinze, and L W. Braile. "The Role of Rifting in the Tectonic Development of the Midcontinene, U.S.A." *Tectonophysics* 94 (1983): 391-412.

Killian, B.J., 2012, Sequence Stratigraphy of the Woodford Shale, Anadarko Basin, Oklahoma: Implications on Regional Woodford Target Correlation: M.S. thesis, University of Oklahoma, Norman, OK, 102p.

Mann, E., 2014, Stratigraphic Study of Organic-Rich Microfacies of the Woodford Shale Anadarko Basin, Oklahoma: M.S. thesis, University of Oklahoma, Norman, OK, 122p.

McCullough, B.J. 2014, Sequence stratigraphic framework and characterization of the Woodford Shale on the southern Cherokee Platform of central Oklahoma:. M.S. thesis, University of Oklahoma. 212pp.

Miceli-Romero, A. A., 2010, Geochemical characterization of the Woodford Shale, Central and Southeastern Oklahoma: M.S. thesis, University of Oklahoma, Norman, OK, 133p.

Mitchum, R., M., Jr., Van Wagoner, J., C., 1990, High-frequency sequences and eustatic cycles in the Gulf of Mexico basin: Proceedings, Gulf Coast Section SEPM 11th Annual Research conference, p. 257–267.

Molinares, C., 2013, Stratigraphy and palynomorphs composition of the Woodford Shale in the Wyche Farm Shale pit, Pontotoc County, Oklahoma: M.S. thesis, University of Oklahoma, Norman, OK, 90p.

Portas, R., 2009, Characterization and origin of fracture patterns in the Woodford Shale in southeastern Oklahoma for application to exploration and development: M.S. thesis, University of Oklahoma, Norman, OK, 113p.

Serna-Bernal, A., 2013, Geological Characterization of the Woodford Shale McAlister Cemetery Quarry, Criner Hills, Ardmore Basin, Oklahoma: M.S. thesis, University of Oklahoma, Norman, OK, 141p.

Tran, M.H., 2009, Geomechanics Field and Laboratory Characterization of Woodford Shale: M.S. thesis, University of Oklahoma, Norman, OK, 103p.

Treanton, J., 2014, Outcrop-Derived Chemostratigraphy of the Woodford Shale, Murray County, Oklahoma: M.S. thesis, University of Oklahoma, Norman, OK, 83p.

Turner, B.W., Treanton, J.A., and Slatt, R.M. “The Use of Chemostratigraphy to Refine Ambiguous Sequence Stratigraphic Correlations in Marine Mudrocks. An Example from the Woodford Shale, Oklahoma, USA.” *Journal of the Geological Society*, **173** (2016), 854-868.

Zalasiewicz, J., Smith, A., Brenchley, P., Evans, J., Knox, R., Riley, N., Gale, Al., Gregory, F.J., Rushton, A., Gibbard, P., Hesselbo, S., Marshall, J., Oates, M., Rawson, P., & Trewin, N. 2004. Simplifying the stratigraphy of time. *Geology*, **32**, 1-4.

Appendix: Map Variants

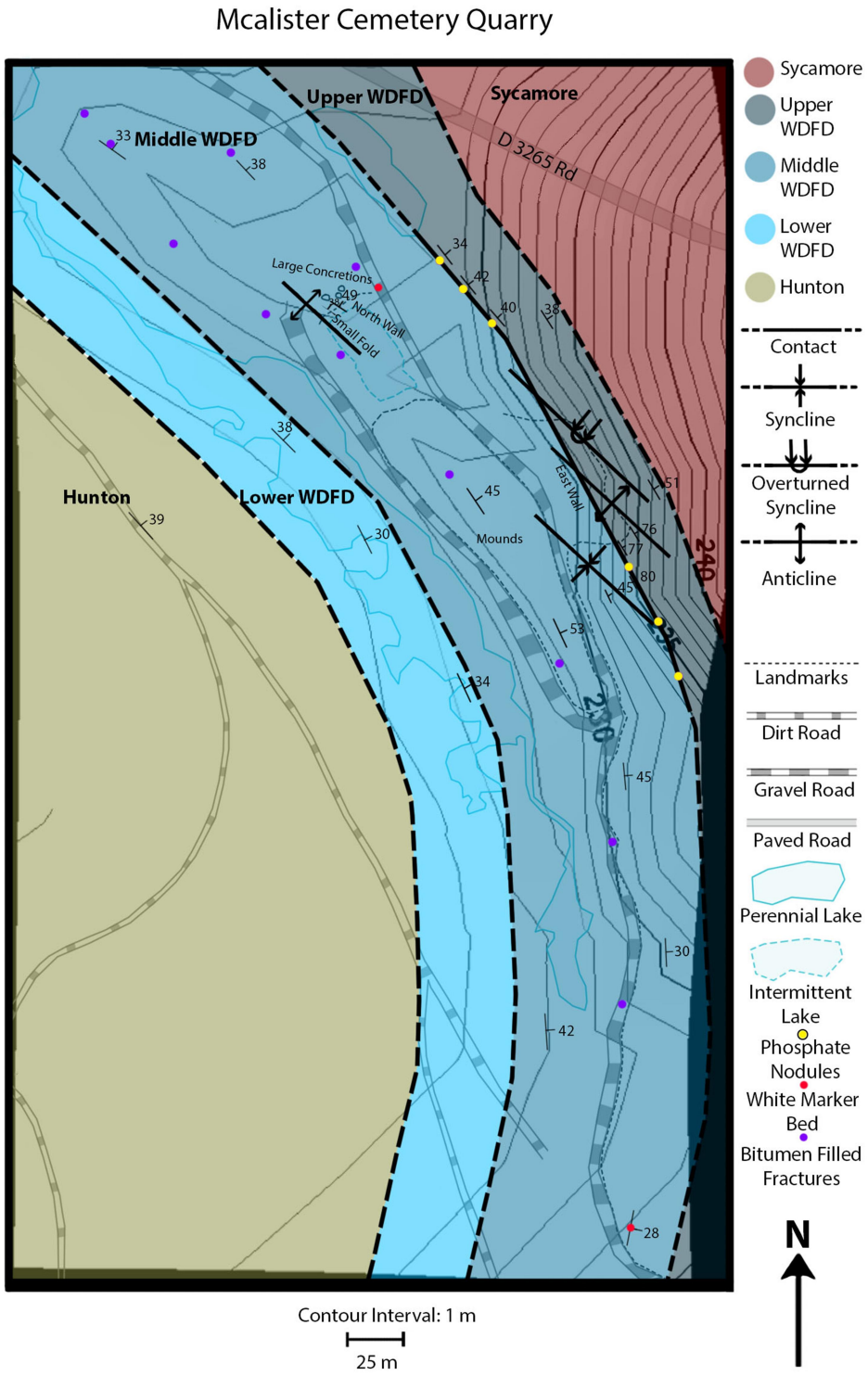

This map is included for anyone who might visit the quarry to take notes on. It includes the topographic data and major landmarks, however the Google aerial photo has been removed from the image to simplify it for field use.

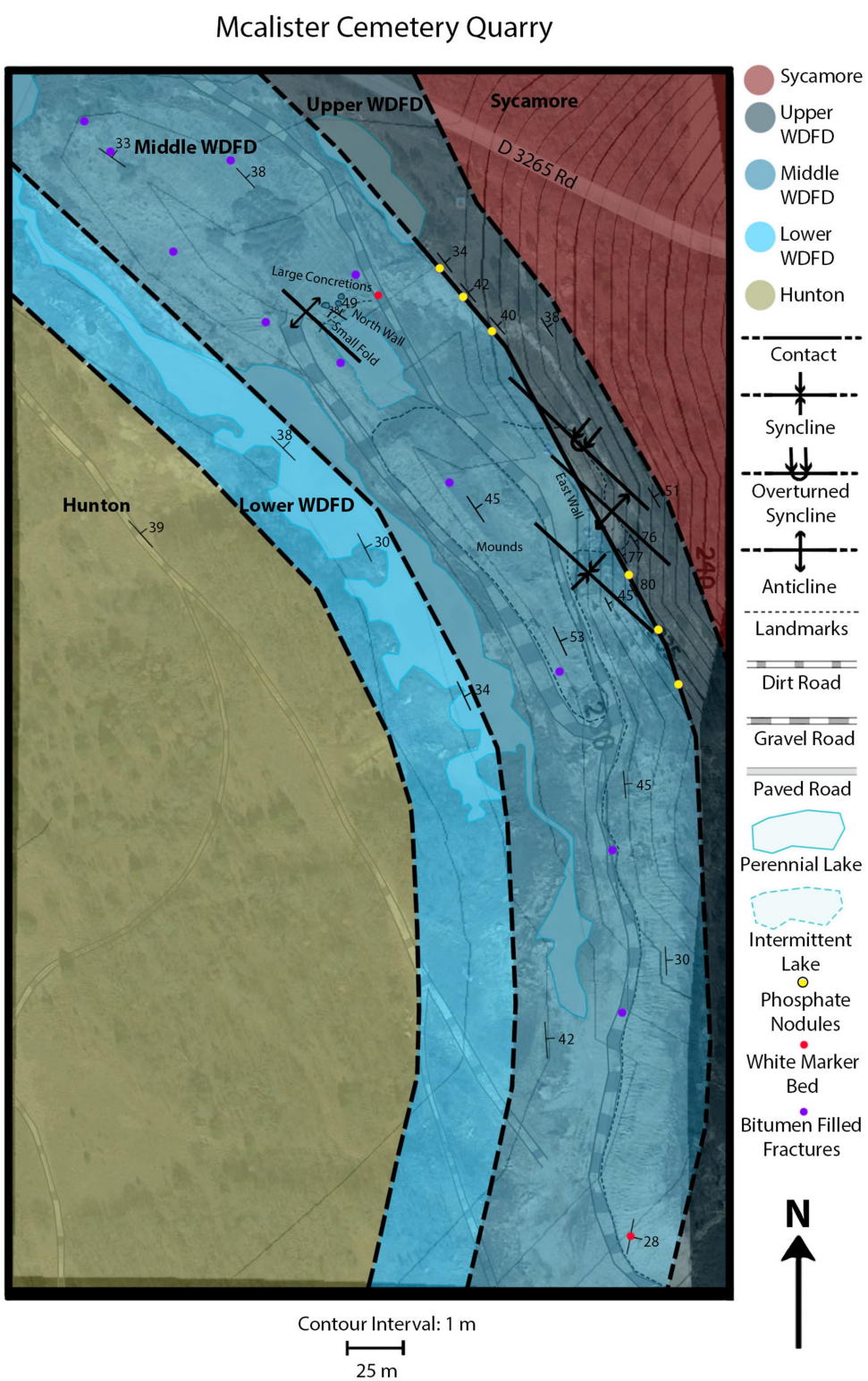

This map is included for anyone who might visit the quarry to take notes on. It includes the topographic data and major landmarks, as well as Google aerial imagery.